ELSEVIER

Contents lists available at ScienceDirect

Scientific African

journal homepage: www.elsevier.com/locate/sciaf





Experimental drying characteristics of a portable solar dryer for apple slices in consecutive and continuous tests

Patrick Tsopbou Ngueagni, Ashmore Mawire *

Material Science, Innovation and Modelling (MaSIM) Research Focus Area, North-West University, Mmabatho 2745, Mahikeng, South Africa

ARTICLE INFO

Editor: DR B Gyampoh

Keywords:
Apple slices
Portable solar dryer
Consecutive and continuous tests
Drying Kinetics
Mathematical Models

ABSTRACT

A portable solar dryer constructed with cost-effective materials, operated in sunny and cloudy conditions for off-grid farmerswas successfully used for extending the shelf life of apple slices in three different experiments. The performance of the portable dryer was evaluated in three 8-hour consecutive and three 32-hour continuous drying tests. Parameters that influenced the dryer's performance were the solar radiation, relative humidity, wind speed, and drying temperatures. The top tray exhibited the lowest final moisture ratio with a drying time of around 10 h, and a final RH of around 16 %. The average drying rates were 0.050, 0.058, and 0.066 kg/h, whereas the maximum values of specific energy consumption (SEC) were 8.31, 12.02, and 15.10 kWh/kg for three 8-hour tests. The effective moisture diffusivity (Deff) values of dried apple slices were 1.89×10^{-10} , 1.68×10^{-10} , and 1.78×10^{-10} m 2 /s for the three 8-hour tests. The rehydration ratios (RR) values were 3.10, 3.25, and 3.31, while the shrinkage factors were found to be 43.2, 42.64, and 41.36 %. Modelling showed that the Page model with an average R² value of 0.9985 was the best fit to describe and predict the drying behaviour of apple slices. In the 32-hour drying test, the weather conditions affected the thermal profiling of trays and walls during daytime, while temperatures of the dryer's components were lower than the ambient temperature at night. The final moisture ratios were 0.1029, 0.0971, and 0.0857 on the top trays, while the SEC was 10.30, 10.86, and 11.38 kWh/kg for the drying tests.

Introduction

The growing world population and urban development are undeniably linked to the massive increase in nutritional needs, affecting the quality, preservation, and storage of food products, especially fruits and vegetables. According to a Food and Agriculture Organization (FAO) report, about 14 % of the world's food production is lost throughout the global supply chain from harvesting to the consumers due to post-harvesting losses [1]. In rural areas, inadequate and poor storage facilities after harvesting agricultural products lead to deterioration, reducing their supply and profitability, and triggering price increases. To tackle this issue, numerous large-scale processing methods, including canning, freezing, drying, fluidized bed, microwave drying, and dehydration, have been widely implemented in developed countries to improve food security and maximise profits [2,3]. Solar drying is an environmentally friendly, readily available, cost-free method that has been used for centuries to preserve food quality in ambient conditions. It prevents enzymatic and microbiological growth, quality deterioration during storage, and extends the product's shelf life by reducing its moisture content up to an optimum level while preserving the nutritional value of food [4]. Its renewable nature and the energy and

E-mail address: ashmore.mawire@nwu.ac.za (A. Mawire).

^{*} Corresponding author.

Nomenclature Abbreviation MR Moisture ratio RHRelative humidity DR Drying rate SEC Specific energy consumption, Kwh/kg OSD Open sun drying PVPhotovoltaic ISTD indirect type solar drying wh Wet basis Symbols Area, m² Α C_{pa} Heat specific capacity of air, kJ/kg °C ḿа Mass flow rate of air, kg/s m_{ia} Initial mass of apple slices, kg Final mass of apple slices, kg mif Q heat supply (W) $h_1, h_2, ..., h_n$ Independent parameters v₁, v₂,..., v_n Uncertainties of measured parameters Greek symbols Efficiencies, % Reduced Chi-square Subscripts Ambient temperature, °C Amb Top wall tw tr1 Top tray tr2 Upper-middle tray Lower-middle trav tr3 tr4 Bottom tray coll collector

mass transfer involved in the process are key factors attracting researchers. This complex process involves uneven heat and mass transfer, as well as physical and chemical changes that can influence the quality of the final product.

In developing countries, especially in rural or resource-limited regions where electricity access is expensive or unreliable, most people rely on open sun drying (OSD) methods for drying their agricultural products. This traditional technique, used since ancient times, is simple to operate, scalable, cost-effective, and requires minimal maintenance. However, large-scale application of this method faces several limitations, including: (i) procedures that are labour-demanding and monitoring for a long period for a wide area are necessary, (ii) a non-repeating drying process under unfavourable weather circumstances, (iii) dried food is susceptible to contamination by animals or insects, (iv) high labour intensive processing, and (v) re-absorption of moisture on the dried food during non-shine periods [5,6]. Within the scope of long-term sustainability, overcoming the above limitations and satisfying the huge demand for good quality dried food products, the indirect type solar drying (ISTD) has emerged as a promising alternative in terms of performance and drying kinetics compared to infrared, radio frequency, vacuum, freeze, and microwave dryers. In this approach, solar air collectors transfer thermal energy into the drying chamber, and hot air facilitates the removal of moisture content from food products [7]. Consequently, the performance of various specified solar drying systems has been extensively studied to examine their efficiency, drying characteristics, and integration into post-harvest management on farms. Different configurations of direct, indirect, and hybrid dryers have been designed and tested for drying numerous fruits, including bananas [6], tomatoes [8], kiwifruit [9], grapes [10], apples [11–13], and date fruits [14].

Malus domestica, commonly known as apples, is among the most popular fruits worldwide, producing about 81 million metric tons throughout all seasons [15]. Apples are typically eaten fresh as a healthy, popular snack rich in antioxidants, vitamins (A and C), and fiber, or processed into products like jam or juice [15,16]. However, due to their significant water content (80-85% on the wet basis (w.b)), apples are highly perishable, reducing their shelf life and affecting the income stability of farmers, productivity, long-term farming, and resilience. The need to provide adequate solutions has emerged in numerous research works to improve the functionality and efficiency of solar dryers to dry apple slices. The effects of convective drying (CD) and microwave drying (MD) on the characteristics of apple slices at different temperatures (50, 60, and 70 °C) and microwave (90, 180, 360 W) were studied by Sharabiani et al. [17]. It was found that with a constant air velocity of 1 m/s, the lowest drying time in MD was 50 min at 360 W, whereas 100 min was obtained at 70 °C for CD. Moreover, the maximum effective moisture diffusivity was 4.07×10^{-7} and 8.21×10^{-7} m²/s for CD and

MD, respectively. In a recent study Mesery et al. [18]. evaluated the drying of apple slices and quality attributes of apple slices under different infrared intensities (0.130 to 0.341 W/cm 2), air velocities (0.5 to 1.5 m/s), and thicknesses (2 to 6 mm). The results showed that the drying time needed to decrease the moisture level of sliced apples to roughly 0.12 g water/g on a dry basis ranged from 200 to 280 min, 170–240 min, and 130–190 min. The rehydration ratio increased with the increase in the air velocity but decreased with increased infrared radiation intensity. However, a contrasting phenomenon was observed for the shrinkage ratio. Lingayat et al. [19] developed an ITSD with a V-shaped absorber plate, and air flowing upwards through four plastic trays. The average temperature at the collector outlet was 58.63 °C with a decrease in the moisture content of up to 87 %, and an average effective moisture diffusivity of 4.28×10^{-9} m 2 /s.

The exergy and energy assessments within dryers and solar air heaters (SAHs) over two days were evaluated by Kidane et al. [20]. The average efficiencies of 53.85 and 49.79 % for two different solar air heaters on day 1 were obtained, respectively, while values of 37.94 and 36.15 % were obtained for dryers. In another study using solar air heaters on two loads of sliced apples, Kidane et al. [13] showed that the average efficiency of two different dryers at half capacity was 11.69 % and it was was 22.53 % at full capacity, while dryer 1 achieved 12.07 and 23.50 % at half and full capacity, respectively. By investigating the performance analysis of a double-pass solar air dryer (DPSAD) and an infrared (IR) assisted double-pass solar air dryer (DPSAIRD) of apple slices, it was proven that IR dryer significantly increased the specific energy consumption (SEC), while the DPSAIRD resulted in exergy losses 45 % larger than the DPSAD [21]. Likewise, the highest thermal efficiency of the collector obtained in summer was 83.56 %, while energy efficiencies ranged between 2.20 % and 26.46 % for the DPSAD, 1.15 % and 8.59 % for the DPSAIRD. [New Paragraph joint sentence with the next one]A combination of different methods was also investigated by some researchers.

The hot air flow method showed a longer drying time for apple slices than the microwave method, and the combination of each method [22] . According to the results, the hybridized method resulted in a minimum drying time of 17 min, and the microwave method required a minimum energy consumption of 2684 kJ. Similarly, a pretreatment of apple slices with infrared (IR) and microwave (MW) drying , followed by normal hot air (HA) and low humidity air (LHA) drying at 40 °Cwas studied by Shewale et al. [23]. The combination of the methods was effective for reducing the energy requirement by 37.1 %, drying time by nearly 28 %, reducing shrinkage from 60 to 65 %, and developing porosities ranging from 0.38 to 0.45. Other applications of solar drying were developed through an indirect forced convection solar dryer using solely or combined sensible heat storage medium (SHSM) and phase change materials (PCM) for the drying of medicinal herbs such as *Valeriana Jatamansi* [24–26]. The mean value of exergy efficiency was found to be 30.28 %, the specific energy consumption was 11.33 kWh/kg, and a drying rate of 0.051 kg/h, and a drying time of 120 h were obtained.

From the previous studies, drying parameters such as temperature within the drying chamber, air velocity, and airflow rate are controlled and set constant, which is unfortunately not true in real-drying conditions. Moreover, these dryers with complicated designs are mounted at a fixed position, limiting their accessibility for scattered rural communities, thus affecting the quality of products harvested far from the drying site. Such dryers are hardly adequate for off-grid areas, especially in Africa, and may be underutilized, representing a waste of investment when the quantity of the harvested products is low. When designing dryers for remote areas, simplicity, mobility, portability, fast fabrication, adaptability to various environmental conditions, reduced dependency on fuel or electricity, lower operational costs, and increased farmer revenue are key considerations. Such dryers should be constructed using local materials and tailored to community needs. Promoting such integrated thermal solar dryers (ITSD) without technical expertise supports rural development and economic sustainability in Africa. To the best knowledge of the author's, very limited studies have been conducted on the performance of portable ITSDs in the convection mode with downward-blowing fans for continuous (8-hour test) and consecutive (32-hour) drying of apple slices in real-world conditions. Moreover, no study has emphasized the effect of thermal profiling of the walls on the temperature within the drying chamber, which is required for a more comprehensive understanding of the drying kinetics of apple slices. Additionally, solar drying studies of apples in a portable dryer are limited. This work addresses those gaps and presents a novel portable dryer for apple slices which can also be used for drying other food products. This study aims to evaluate the performance and quality attributes of a standalone portable solar dryer with integrated downward-blowing fans. The investigation examines drying kinetics (moisture ratio, drying duration, relative humidity, and drying rate), thermal properties, and overall performance in consecutive and continuous tests. Additionally, twelve mathematical models are used to accurately predict the drying behaviour of apple slices. Finally, energy consumption and quality parameters such as shrinkage, rehydration, and ratio coefficients are assessed. Based on the experimental results, the proposed portable solar dryer could be a significant step forward in developing automated, cost-effective solar dryers for small-scale users or farmers in remote areas for usage in consecutive and continuous drying tests.

Materials and methods

This section presents the preparation, experimental setup, drying characteristics, quality assessment, and mathematical modelling for the experiments.

Collection and processing of fresh apples

Fresh and ripe apples were purchased from a local supermarket in Mafikeng, South Africa. Prior to the experiment, the fruits were carefully selected in terms of uniformity of size and colour. The apples were then thoroughly washed with tap water to remove dirt, dust, or other particles from transporting or handling. A sharpened kitchen knife was used to slice the apples into circular shapes of approximately 3.6 ± 0.1 mm thickness, followed by removing the seeds and adding lemon juice to prevent color changes during the

drying process. Next, 350 g of apple pieces were weighed with a digital balance, and evenly spread across four metallic trays, in the drying chamber.

Description of the experimental setup

(latitude 25.8253° N; longitude 25.6097° E). The main components of the drying system include a drying chamber, two batteries, a solar collector, a datalogger, and a hygrometer. Figs 1 and 2 show the photograph and a schematic diagram of the experimental setup, respectively. The drying chamber is made of stainless steel, black painted, and consists of glazing material at the top wall chosen for its high solar transmittance, rigidity, and to allow sunlight to get inside the drying cabinet. Two DC fans are located at the top wall of the drying chamber to continuously blow warm air inside the dryer and get rid of moisture from sliced apples over time via small holes located at the bottom wall. The DC fans were powered by a set of two 12 V batteries connected to a charge controller that regulates the voltage and current flowing from the solar panel to the batteries. Four metallic wire mesh trays (5 cm thickness and 0.683 kg each) were manually placed inside the drying chamber at an equidistance of 5 cm between them to allow the air to interact with the apple slices to be dried. K-thermocouples were chosen in this study because of their fast response, local availability, adaptability, flexibility and their resistance to corrosion and oxidation at the required drying temperatures. The thermocouples were placed in the middle of each tray and connected to a datalogger to monitor the temperature throughout continuous and consecutive drying tests. Three thermocouples were also placed on the top, left, and right walls of the drying chamber to measure the wall temperatures and evaluate the effect of absorbed heat on drying apple slices. Apple slices were placed on the trays carefully in the drying chamber by hand. The data of moisture reduction were recorded with a hygrometer permanently placed inside the drying chamber. The whole experimental setup was placed on a table and exposed to a sunny area. The details of different components of the dryer are given in Table 1.

Experimental procedure and instrumentation

Experiments were conducted under outdoor conditions from September to October 2024 to evaluate the performance of the proposed system. Experimental tests with apple slices were performed as two 8-hour consecutive tests (from 09:00 am to 17:00 pm on the same day) and 32-hour continuous tests (from 09:00 am on the first day to 5:00 pm of the next day). Each drying test was performed thrice, and results were expressed as a mean \pm standard deviation. Temperature measurements in the portable dryer were measured using K-thermocouples positioned at various locations on the drying system, and one was used to monitor the ambient temperature. All the thermocouples were then connected to a datalogger using a 20-channel multiplexer adapter. The temperatures were recorded in ten-second intervals during the experiments. The outdoor temperature, humidity, and airflow velocity were recorded with a weather station, oriented eastward, while the airflow rate and wind speed were measured using a hot-wire anemometer. The relative humidity (RH) of the drying air inside the drying cabinet was measured with a hygrometer. Global solar radiation was measured using a pyranometer placed on the laboratory roof in ten-second intervals. The loss of moisture content was evaluated by measuring the mass of partially dried apple slices every hour. Table 2 displays the specifications of the instruments used during the drying tests.

Experimental uncertainties

The accuracies of measurement instruments were used to calculate the uncertainty of the measured parameters $(v_1, v_2, v_3, ..., v_n)$. The independent/measured parameters $(h_1, h_2, h_3, ..., h_n)$ determine the dependent parameter (D). The dependent parameter's (UD) uncertainty is computed using Eq. (1):

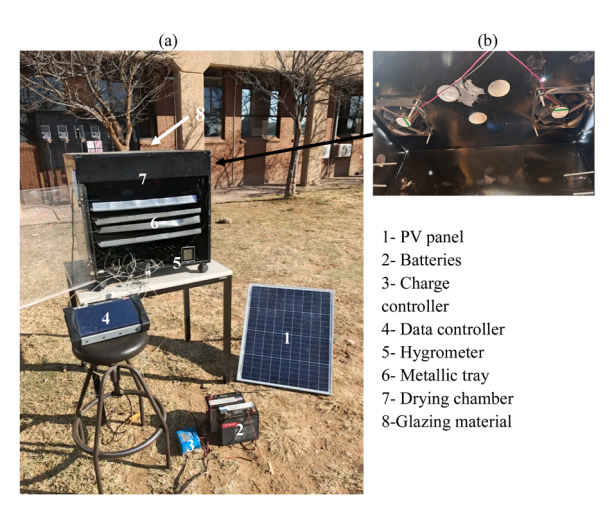


Fig. 1. A photograph of (a) experimental setup and (b) top view of fans in the dryer.

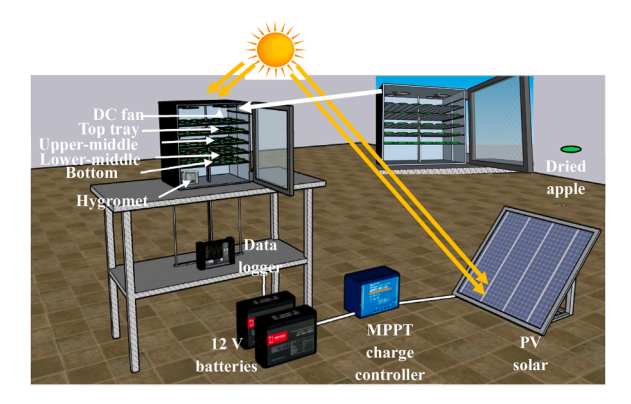


Fig. 2. Schematic diagram of the indirect solar dryer with upside view of DC fans on the top wall.

Table 1Components and specifications of the indirect solar dryer.

Components	Specifications	Manufacturers
Drying chamber	Stainless steel, $450 \times 600 \times 560$ mm, Mass= 4.2 kg	Custom made
Glazing material	Borosilicate, 0.5×0.5 m, thickness 5mm	/
Solar PV panel	P_{max} =50 W, Vmp=18.1 V; Isc=2.94 A; Imp=2.77 A Dimensions=6.70×5.30×0.025 m, $E = 1000 \text{ W/m}^2$	SOSOLAR
Charge controller	PV=100 V; 12/24/48 V; 25A - 35 A	Victron Energy
Tray	Dimensions: 0.051×0.047 m, thickness= 5 cm	Custom made
Battery	LiFePO ₄ , 18Ah, 230.4 Wh, Max. current=18 A,	Red pole energy
Fan	Lead wire, Speed=3100 rpm, $120 \times 120 \times 25$ mm, DC=12 V, Power=5.40 W	SUNON

Table 2Instruments used during the drying tests and their specifications.

Measurement devices	Specifications/Manufacturers	Range	Accuracy
Temperature	K-type / PRO	−50 to 600 °C	± 0.15 °C
Pyranometer	CMP11 / Kipp and Zonen	0 to 2000 W/m^2	$\pm 10~\text{W/m}^2$
Hygrometer	TP55 / ThermoPro	10–99 %	$\pm 2~\%$
Hot wire anemometer	450i /	0 to 30 m/s	± 0.01 m/s
Weighing balance	CS2000 / OHAUS	0 to 520 g	$\pm~0.001~\mathrm{g}$
Data logger for solar radiation	34972A / Keysight	/	/
Data logger for temperatures	DAS240 / SEFRAM	−250 −1370 °C	±0.5 °C
Weather station	HP2551CA	/	/

$$U_D = \left[\left(\frac{\partial D}{\partial h_1} \nu_1 \right)^2 + \left(\frac{\partial D}{\partial h_2} \nu_2 \right)^2 + \left(\frac{\partial D}{\partial h_3} \nu_3 \right)^2 + \dots + \left(\frac{\partial D}{\partial h_n} \nu_n \right)^2 \right]^{1/2}$$
(1)

The detailed parameters of the measuring instruments, along with their corresponding uncertainty results, are presented in Table 3.

Drying characteristics and modelling of apple slices

Moisture content

The wet basis moisture content of the apple samples was measured using a wet basis method. In the portable solar dryer, the

Table 3 Uncertainty of instruments.

Parameters	Units	Uncertainties
Solar radiation	W/m ²	±14.1
Ambient temperature	°C	± 0.21
Temperature of the drying chamber	°C	± 0.21
Relative humidity	%	± 2.82
Mass measurement of fruit slices	kg	± 0.001
Airflow velocity	m/s	± 0.01
Airflow rate	m ³ /h	± 0.01
Final moisture content	-	± 0.01

moisture content at different time intervals was determined by the ratio of the mass of water evaporated to the initial mass of the apple slices. Before drying, 350 g of the samples were weighed, until the end of the experiment. Thehe samples were weighed again every 1 hour to assess the moisture loss during the 8 -hour tests. The moisture content us is expressed using Eq. (2) as:

$$MC = \frac{m_{ia} - m_{fa}}{m_{ia}} \tag{2}$$

where MC is the Moisture content rate (% wet basis) at a given time, mia and mfa are the weight (kg) of the wet and dry apple slices

Moisture ratio

The dry-weight basis approach was used to estimate the food drying rate, defined as the rate at which moisture was removed from the drying food product. The dimensionless moisture ratio values were evaluated at different time intervals by using Eq. (3):

$$MR = \frac{M_t - M_{eq}}{M_0 - M_e} \tag{3}$$

where t is the drying time (hour), MR is the moisture ratio, M_0 , M_{eq} , and M_t are the starting, equilibrium, and moisture content at time "t", respectively. For practical purposes in thin layer drying, equilibrium moisture content is small and negligible [27]. Moreover, as temperature and the relative (RH) values inside the chamber were continuously varying throughout the experiments, Eq. (3) can be simplified to:

$$MR = \frac{M_t}{M_0} \tag{4}$$

Drying rate

The drying rate (DR) of a food product quantifies the volume of water evaporated per unit time during the drying process [28]. It can be measured in kg/h using the expression in Eq. (5).

$$DR = \frac{M_1 - M_2}{t_1 - t_2} \tag{5}$$

where M_1 and M_2 are the initial and ending weights (kg) of apple slices, respectively. t_1 and t_2 are the definite drying times in hours (h) to dehydrate the samples from M_1 and M_2 .

Effective moisture diffusivity and activation energy

The simplified Fick's second law, also known as Fick's diffusion equations, can be used to evaluate the water diffusivity of biological compounds by neglecting shrinkage [29]. The effective moisture diffusivity is a crucial transport characteristic of food products for estimating the amount of moisture that moves on their surface. Fick's second law is represented by the following expression (Eq. (6)).

$$MR = \frac{M_t - M_{eq}}{M_0 - M_e} = \frac{8}{\pi^2} \sum_{n=1}^{\infty} \frac{1}{n^2} \exp\left(-\frac{n^2 \pi^2 D_{eff} t}{4L^2}\right)$$
 (6)

where D_{eff} is the effective moisture diffusivity (m²/s), L is the thickness of apple slices (m), n is the positive integer, and t is the drying time (s).

By considering the long-term during times (n = 1), the linearized and simplified diffusion description [30] is given using Eq. (7) as:

$$\ln MR = \ln \left(\frac{8}{\pi^2}\right) - \left(\frac{\pi^2 D_{eff} t}{4L^2}\right) \tag{7}$$

The effective moisture diffusivity of apple fruits is estimated by analysing the relationship between the natural logarithm of the moisture ratio (ln MR) and time. The slope derived from the linear fitting of the experimental drying data is expressed as follows (Eq. (8)):

$$slope = \left(-\frac{\pi^2 D_{eff}}{4L^2}\right) \tag{8}$$

$$D_{eff} = -\frac{slope}{\pi^2 \cdot 4L^2} \tag{9}$$

Mathematical modelling of drying curves

The conventional drying curve approach describes the drying kinetics of the samples using an empirical equation generated by adapting the drying experimental data of moisture content versus time of each drying test. Several equations are provided in the literature and presented in Table 4 to predict the evolution of dried apple slices during the falling rate period of the drying process and, thereby, determining the best-fit curve. The coefficient of determination (R^2) given by Eq. (10) and Chi-square (χ^2) expressed by Eq.

(11) were used to assess the quality of the adjustment of the chosen model by using the Levenberg-Marquardt approach with the Origin program. These parameters are given by the following equations:

$$R^{2} = 1 - \frac{\sum_{i=1}^{N} (MR_{\text{pre},i} - MR_{\text{exp},i})^{2}}{\sum_{i=1}^{N} (MR_{\text{exp},i})^{2}}$$
(10)

$$\chi^{2} = \frac{\sum_{i=1}^{N} (MR_{pre,i} - MR_{exp,i})^{2}}{N - z}$$
(11)

where $MR_{pre,i}$ is the ith predicted MR, $MR_{exp,i}$ is the ith experimental MR, N and z are the total number of experiments and constants, respectively. Lower $\chi 2$ and higher R^2 represent the perfect fitting to the model from the experimental data.

Investigation of performance parameters

Solar collector efficiency

The performance of the collector, expressed as collector efficiency (η_{coll}) is evaluated as the ratio of useful heat output of the collector (Q_u) to the heat input to the collector reported by [42] using Eq. (12) as

$$\eta_{coll} = \frac{Q_u}{Q_i} = \frac{\dot{m}_a C_{pa} (T_{top} - T_{amb})}{I_{sr} A_{coll}} \tag{12}$$

,where T_{top} and T_{amb} represent the temperatures (K) of the top tray and the ambient atmosphere, C_{pa} (J/kgK) the specific heat capacity of air, \dot{m}_a (kg/s) the mass flow rate of the air, I_{sr} (W/m²) the instantaneous solar radiation intensity at a given time, and A_{coll} (m²) the surface area of the dryer.

Specific energy consumption (SEC)

Specific energy consumption (SEC) is determined during the drying process in terms of energy efficiency and cost-effectiveness. It represents the energy required to evaporate one unit mass of water from apple slices (Eq. (13)):

$$SEC = \frac{E_{in}}{m_w} = \frac{I_{sr}A_{coll}t_{dt}}{m_w} \tag{13}$$

where t_d represents the total drying time of the apple sample.

Quality assessment of dried apple slices

Evaluating the quality of the dried apple slices requires the assessment of some key characteristics to ensure compliance with specified requirements, including texture and appearance. In each drying test, the rehydration ratio, shrinkage in volume and diameter, and water activity were determined.

Rehydration ratio

Also known as the rehydration factor, the rehydration ratio (RR) quantifies the ability of a rehydrated product to rehydrate with a specific volume and moisture content using a given amount of water. In this study, RR was evaluated by following the procedure given by Ullah et al. [9]. with slight modifications. Dried apple slices (10 g) were added to 200 mL of distilled water and kept in a water bath at 40 °C for 30 min. The rehydrated sample was then gently blotted on a tissue paper and weighed using a digital electronic scale. Rehydration ratio and coefficient of rehydration are respectively expressed by Eqs. (14) and (15) [43] as:

Table 4Mathematical models used for predicting the thin-layer drying behaviour of apple slices.

Model name	Model equation	References
Newton	MR = exp (-kt)	[31]
Page	MR = exp(-ktn)	[32]
Modified Page	MR = exp(-kt)n	[33]
Henderson-Pabis	MR = aexp(-kt)	[34]
Logarithm	MR = aexp(-kt) + c	[35]
Midili and Kucuk	$MR = aexp(-kt^n) + bt$	[36]
Two-term	$MR = aexp(-k_0t) + bexp(-k_1t)$	[37]
Two-term Exp.	MR = aexp(-kt) + (1 - a)exp(-kat)	[11]
Mod. Henderson Pabis	MR = aexp(-kt) + bexp(-gt) + cexp(-ht)	[38]
Wang-Singh	$MR = 1 + at + bt^2$	[39]
Diffusion approach	MR = aexp(-kt) + (1 - a)exp(-kbt)	[40]
Verma et al.	$MR = a \exp(-kt) + (1 - a) \exp(-gt)$	[41]

$$RR = \left(\frac{W_f}{W_o}\right) X100 \tag{14}$$

$$CR = \frac{W_f X(100 - W_0)}{(W_0 - M_c)X100} \tag{15}$$

where W_0 denotes the weight (kg) of apple slices before rehydration, W_f is the weight (kg) of rehydrated apple slices, and M_c represents the moisture content of dried apple slices before rehydration.

Shrinkage of apples

Shrinkage in dried food products is the loss of their original size, weight, and volume that was wet when they undergo dehydration or desiccation. As the food loses its moisture, it also shrinks in size to become smaller and lighter in size and weight than its original fresh form. Shrinking is an inherent consequence of the drying process, attributable to the substantial proportion of moisture present in numerous food items. Its extraction engenders a condensation of solids, cumulating to a decrease in both size and weight [44]. During the rehydration process, moisture removal affects the change in volume of apples. Likewise, owing to their globose to globose-conical shape, the geometric mean diameter of fresh and dried apples can be measured. The values of shrinkage (S) in diameter are calculated as shown in Eq. (16).

Shrinkage in diameter =
$$\left(\frac{D_0 - D}{D_0}\right) X100$$
 (16)

where D₀ and D represent the initial and final diameters of fresh and dried apple slices, respectively.

Experimental results and discussion

Experiments on drying apple slices were carried out to assess the performance of the portable solar dryer, as detailed in the previous sections. A total of three tests were conducted, and the performance was evaluated. This section presents and discusses the findings derived from the experiments.

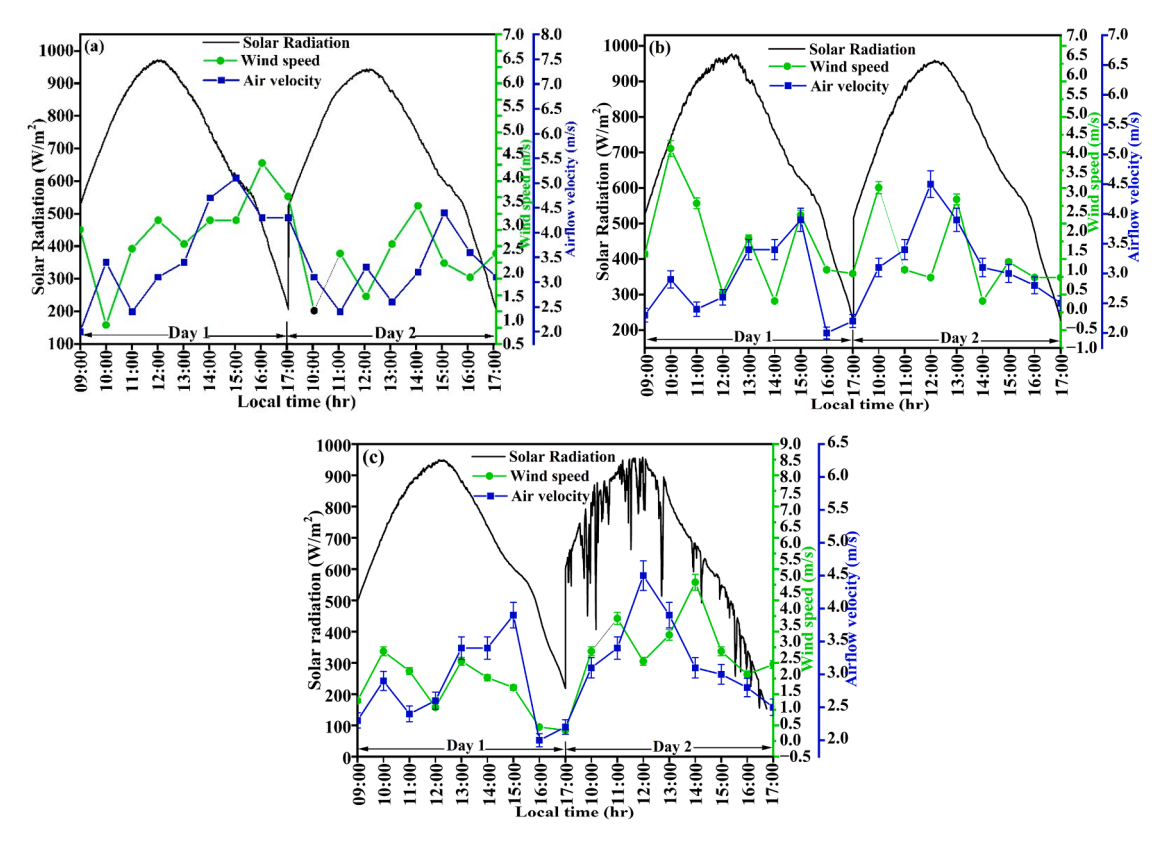


Fig. 3. Hourly evolution of solar radiation intensity, wind speed, and airflow velocity versus time for (a) test 1, (b) test 2, and (c) test 3.

Drying apple slices for consecutive 8-hour tests

Assessment of ambient conditions

Drying experiments were carried out outdoors under sunny and cloudy conditions from 9:00 a.m. to 5:00 pm over two consecutive days from 2-15 September 2024. Fig. 3 depicts the hourly changes in solar radiation, wind speed, and airflow velocity relative to drying time. Notably, wind speed and airflow were not controlled during this study. As shown in the figure, solar radiation gradually increased, peaked around 12:30 pm., and then declined until sunset. From 9:00 a.m. to 12:30 pm. on the first day, solar radiation ranged from 527 to 974 W/m² for test 1, 523 to 981 W/m² for test 2, and 497 to 951 W/m² for test 3. The average solar radiation on day 1 was 723.6, 718.2, and 701.7 W/m² for tests 1, 2, and 3, respectively. These are values are comparable. On day 2, the solar radiation trend was similar for tests 1 and 2, but test 3 showed scattered data due to the recorded cloudy conditions. The average values were 706, 707, and 673 W/m². The lower value for test 3 indicates less favourable weather, consistent with the cloudy conditions observed on day 2. The average solar radiation values are higher than those reported by Tarik et al. [45], suggesting sufficient thermal energy for drying. The hourly variation of wind speed and airflow velocity is also presented, with fluctuations attributed to environmental factors. This observation differs from previous studies [20,21], where most researchers only measured airflow or wind speed at the blower outlet, assuming airflow to be constant and uniform, which is not a true reflection of the drying kinetics inside the drying chamber. The average wind speed and airflow velocity were 2.57, 1.51, and 2.22 m/s for tests 1, 2, and 3, respectively, which are higher than those found by Mawire et al. [6]., who used an indirect solar dryer in the forced convection mode at the same location. Meanwhile, airflow velocities were 3.43, 3.02, and 2.96 m/s in tests 1, 2, and 3, respectively. According to Kushwah et al. [46], uncontrolled airflow can hinder proper heat distribution, leading to uneven drying and inconsistent temperature regulation.

Fig. 4 shows the hourly evolution of air relative humidity versus time over the two consecutive days inside the drying chamber. From 09:00 am to 10:00 am on day 1, an increase in RH was observed from 63 to 68 % for test 1, from 61 to 67 % for test 2, and from 67 to 70 % for test 3 on day 1. These peaks may be due to the combination of high moisture release from apple slices and a slower removal of that moisture from the drying chamber. From 10:00 am to 5:00 pm, a decrease in RH was noticed, showing the removal of moisture from air as it moves within the drying process. From 5:00 pm on day 1 to 11:00 am on the following day, RH increased from 22 to 41 % for test 1, from 21 to 40 % for test 2, and from 23 to 40 % for test 3. This phenomenon can be attributed to the hygroscopic character of partially dried apple slices, which allows the reabsorption of moisture from the air. A similar trend was observed during the evaluation of the performance of solar air heaters and dryers in drying golden apple slices [13]. Hence, the release of newly absorbed moisture increases the relative humidity inside the dryer. On the other hand, moisture within the fruit moves from the damp inner core to the drier outer layers once drying is completed. Consequently, even in the absence of external moisture, the outer layers get more humidity. From 12:00 pm to 5:00 pm on day 2, the constant RH of all the tests may be due to the equilibrium state between the rate of evaporation from apple slices and the rate of moisture removal by airflow.

Fig. 5 (a-c) shows the variations in temperature of the top wall (T_{tw}) , top tray (T_{tr1}) , upper-middle tray (T_{tr2}) , lower-middle tray (T_{tr3}) , bottom tray (T_{tr4}) , and ambient temperature (T_{amb}) , respectively. In all the drying tests, it was observed that the temperature profiles increase or decrease according to the variation of solar radiation. The temperature profiles in the trays for the reported solar dryer system depict characteristic thermal gradients influenced by the position of the drying components relative to the glazing material. For instance, the top walls experience higher temperature profiles in tests 1, 2, and 3 due to their ability to receive significant solar radiation. Warm air circulated from DC fans attached to the top wall moves from the top to the bottom trays. The temperature profiles decrease gradually as moisture is transferred from the apple slices on each tray, resulting in some loss of thermal energy. The values of average ambient temperature were 22.72 and 26.26 °C for test 1, 24.64 and 27.50 °C for test 2, and 25.39 and 26.81 °C for

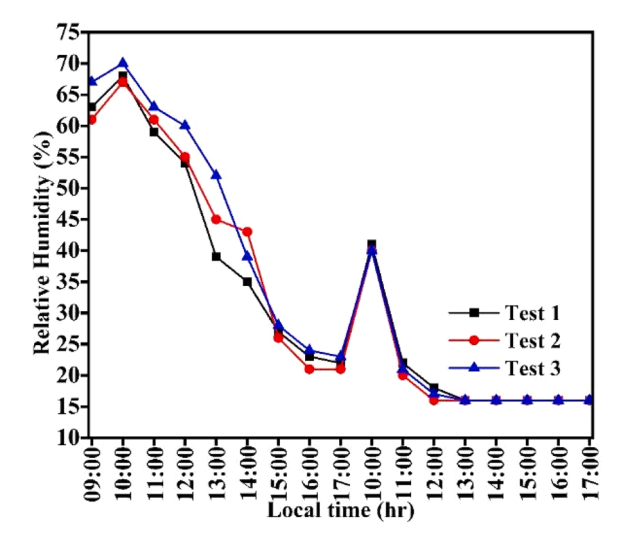


Fig. 4. Relative humidity within the dryer during tests 1, 2, and 3.

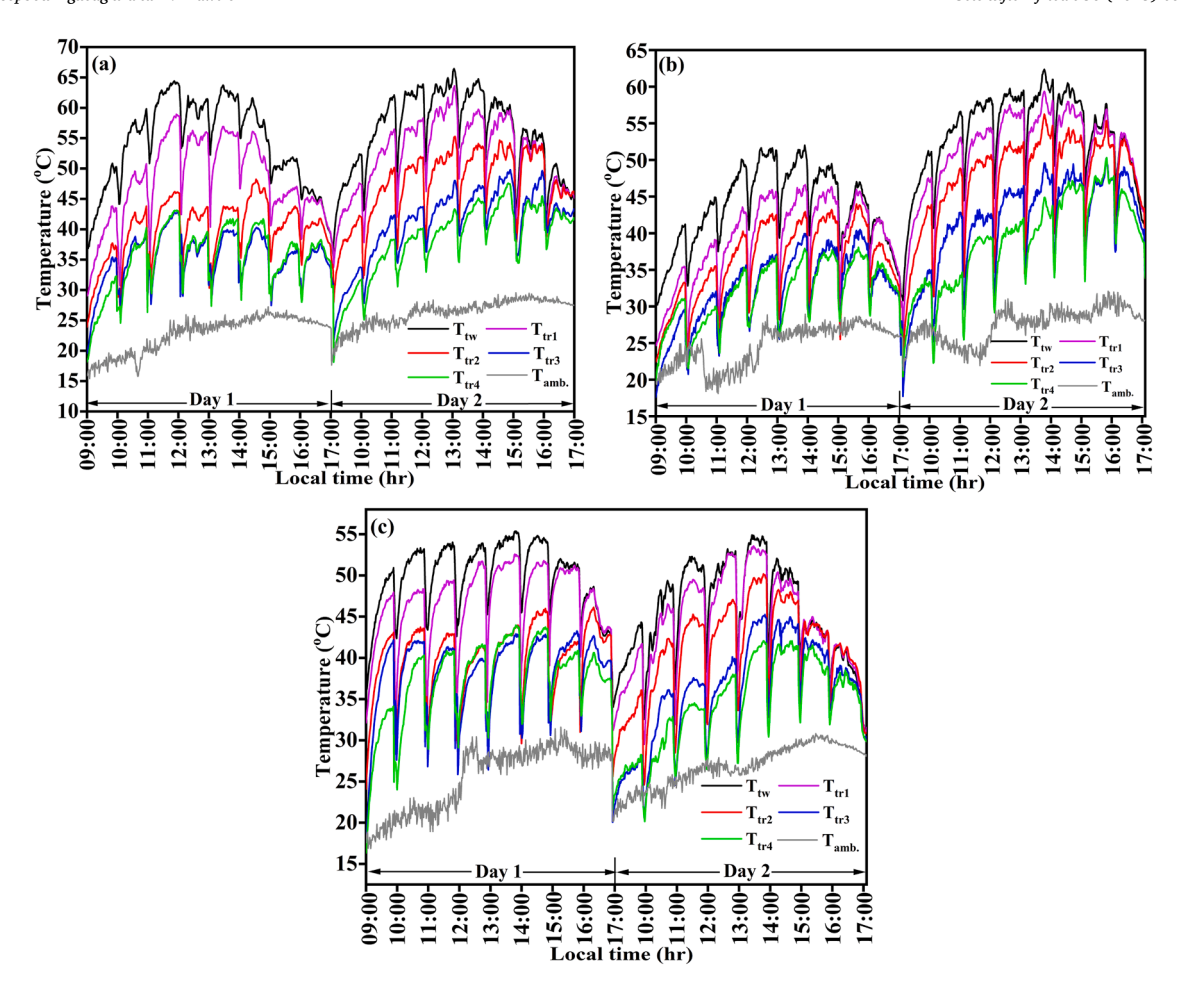


Fig. 5. Temperature distribution of trays and top walls inside the drying chamber during drying of apple slices on (a) test 1, (b) test 2, and (c) test 3.

test 3 during the consecutive drying days, respectively. These values are significantly lower than those of trays. The average temperatures of the top walls were 53.98 and 55.89 °C for test 1, 43.39 and 53.52 °C for test 2, 49.89 and 45.48 °C for test 3 for days 1 and 2, respectively. The temperatures on day 2 were higher than those of day 1 for tests 1 and 2, whereas a converse phenomenon was observed in test 3. These observations highly correspond with the intensities of solar radiation, which are consistent with experimental data of sunny (on tests 1 and 2) and cloudy (on day 2 of test 3) conditions. Moreover, maximum temperatures were observed on day 2 with values of 63.33, 59.23, and 53.46 °C °C for tests 1, 2, and 3, respectively. Over the two consecutive drying days, the hourly opening of the door of the drying chamber to measure the weight of the dried fruit slices and assess their moisture levels lead to a rapid decrease in temperature of the trays. After closing the door, the temperatures exhibit a sharp increase from the bottom tray to the top tray in a short time, indicating minimal heat loss within the dryer, which facilitates the ongoing removal of moisture from sliced apples. These observations are in good agreement with the work of Mawire et al. [6]..

The variations of temperature over time for the left, right, and back walls illustrated in Fig. 6, displayed a similar trend during the 8-hour duration of consecutive drying trials. On the first day, temperatures increased rapidly in response to rising solar radiation. Between 9:00 am and 3:00 pm, the back walls consistently recorded the highest temperatures among the three, often surpassing 45–50 °C by midday. The maximum temperatures attained by the back walls were 44.03 °C for test 1, 56.37 °C for test 2, and 59.46 °C for test 3. This phenomenon is likely due to their higher exposure to solar radiation, leading to enhanced thermal energy absorption, implying excellent heat retention. The hourly drop in temperatures on the right and back walls throughout the tests can be related to the opening and closing of the drying chamber for moisture content assessment in the partially dried apple slices. In contrast, temperatures on the left wall exhibited a gradual rise, peaking around 3:30 pm, attributable to partial exposure to sunlight resulting from the sun's angle. Although the right wall exhibited the lowest temperatures due to its position relative to sunset and sunrise, it remained considerably warmer than the surrounding air, with a peak of around 25–30 °C. On the second day, similar temperature trends were noted for all walls. Their temperatures were significantly above ambient conditions, confirming the dryer's effectiveness in capturing and holding heat. However, the wall temperatures recorded in test 3 were lower than those observed in tests 1 and 2, attributed to reduced solar radiation measured that day. The temperatures of the walls play a crucial role in contributing to the thermal energy within the dryer, exceeding the ambient temperature, which is vital for effective drying. This thermal behaviour underscores effective drying conditions,

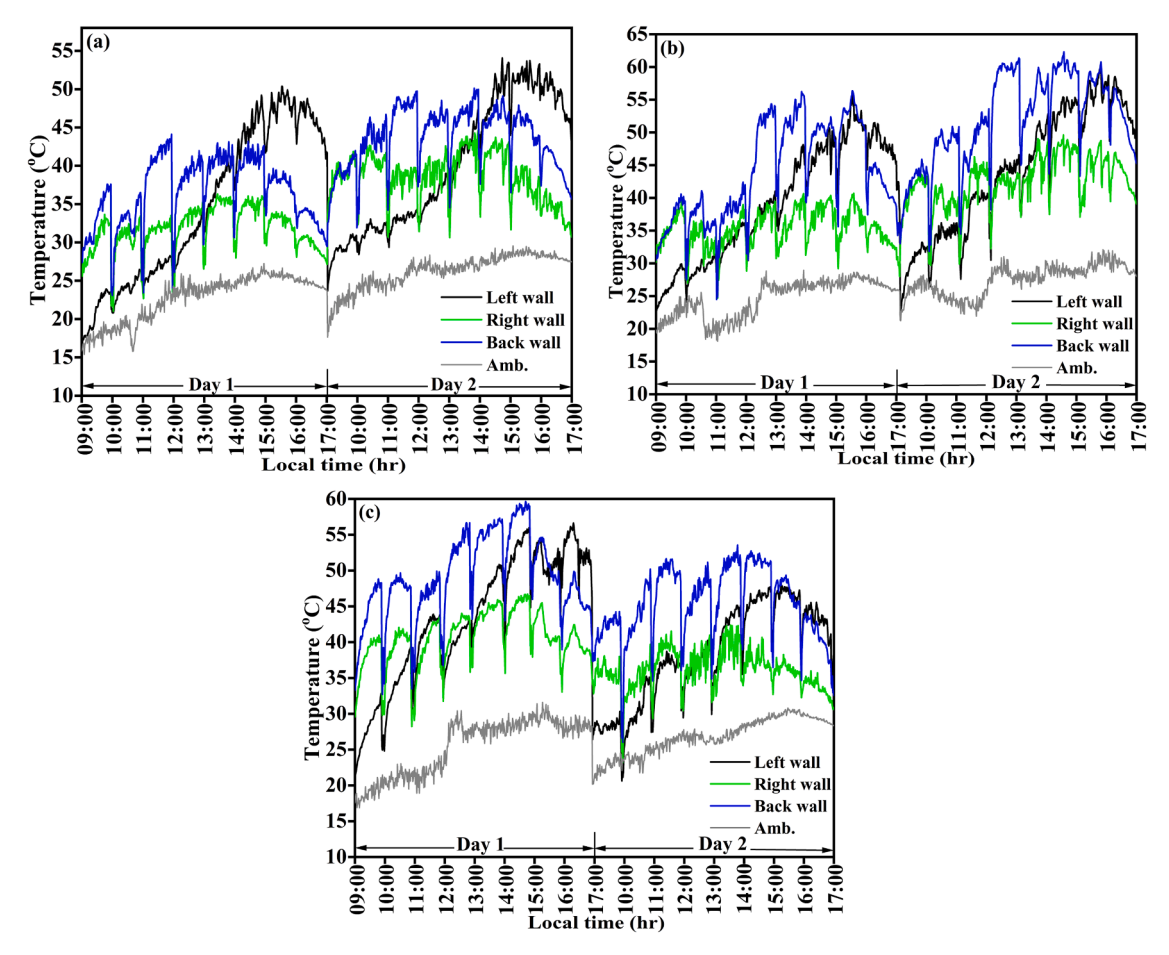


Fig. 6. Hourly temperatures of the walls during the drying of apple slices in (a) test 1, (b) test 2, and (c) test 3.

with the back wall being particularly important in sustaining the internal temperature of the drying chamber.

Drying kinetics analysis of apple slices

The time-dependent change in the moisture ratio profiles of apple slices on a wet basis of the three tests, and the top trays, is shown in Fig. 7(a-d). As expected, the moisture ratio was at its maximum (MR=1) at the beginning of the process and decreased over time in all the trays in different tests. For instance, during test 1, the MR decreases from 1 at 09:00 am to 0.1086, 0.3215, 0.4801, and 0.5258 for top, upper-middle, lower-middle, and bottom trays. Similar findings were observed during tests 2 and 3. This tendency suggests that the drying process effectively reduces the moisture content, which agrees with recent studies conducted by Kidane et al. [13] and Atalay et al. [11], who evaluated the performance and modelling processes of solar drying on apple slices. Notably, it was evident that the top tray performed better compared to the bottom trays. Even though a continuous decrease in the upper-middle, lower-middle, and bottom trays is observed throughout the second day, the MR of the top tray remains nearly constant from 10:00 am–05:00 pm on day 2. This phenomenon could be attributed to the fact that layers of apple slices lose free moisture quickly due to the direct exposure of warm air from DC fans, ensuring rapid evaporation. Then, the moisture from the interior (inner part of the partially dried fruits) must travel a long distance to the surface. This results in a higher moisture removal rate dring the initial stages of drying, which eventually declines with time [47]. A drying time of 10 h (Fig. 6(d)) was obtained for tests 1 and 2 with a MR of 0.0572 and 0.05674, whereas it was 10.5 h for test 3 with a final MR of 0.05143.

The drying rate (DR) refers to the ability of the air to transport moisture across the food product to be dried. Fig. 8(a-c) shows the drying rates of apple slices during tests 1, 2, and 3, while Fig. 8(d) shows the DR of top trays. During the first drying hours of day 1, it was noticed that there was a gradual increase in the DR, attributed to the warming up of the dryer components and the fast evaporation of the outer layer of apple slices. The values of DR recorded in the first trays are higher compared to those of T_{tr2} , T_{tr3} , and T_{tr4} , with maximum values of 0.050, 0.058, and 0.066 kg/h for tests 1, 2, and 3, respectively. These results are consistent with the thermal profiling of the first trays that receive most of the solar radiation from the top wall, hence increasing their temperature and exhibiting a better moisture reduction. On the contrary, from 12:30 pm to 5:00 pm, there was a decrease in the DR. The high values of DR until the end of the first day indicate that the apples are not fully dried due to the free movement of water from the inside to the surface of the apple slices. Over time, water loss reduced porosity, hindering surface migration and slowing drying rates [8]. Furthermore, as

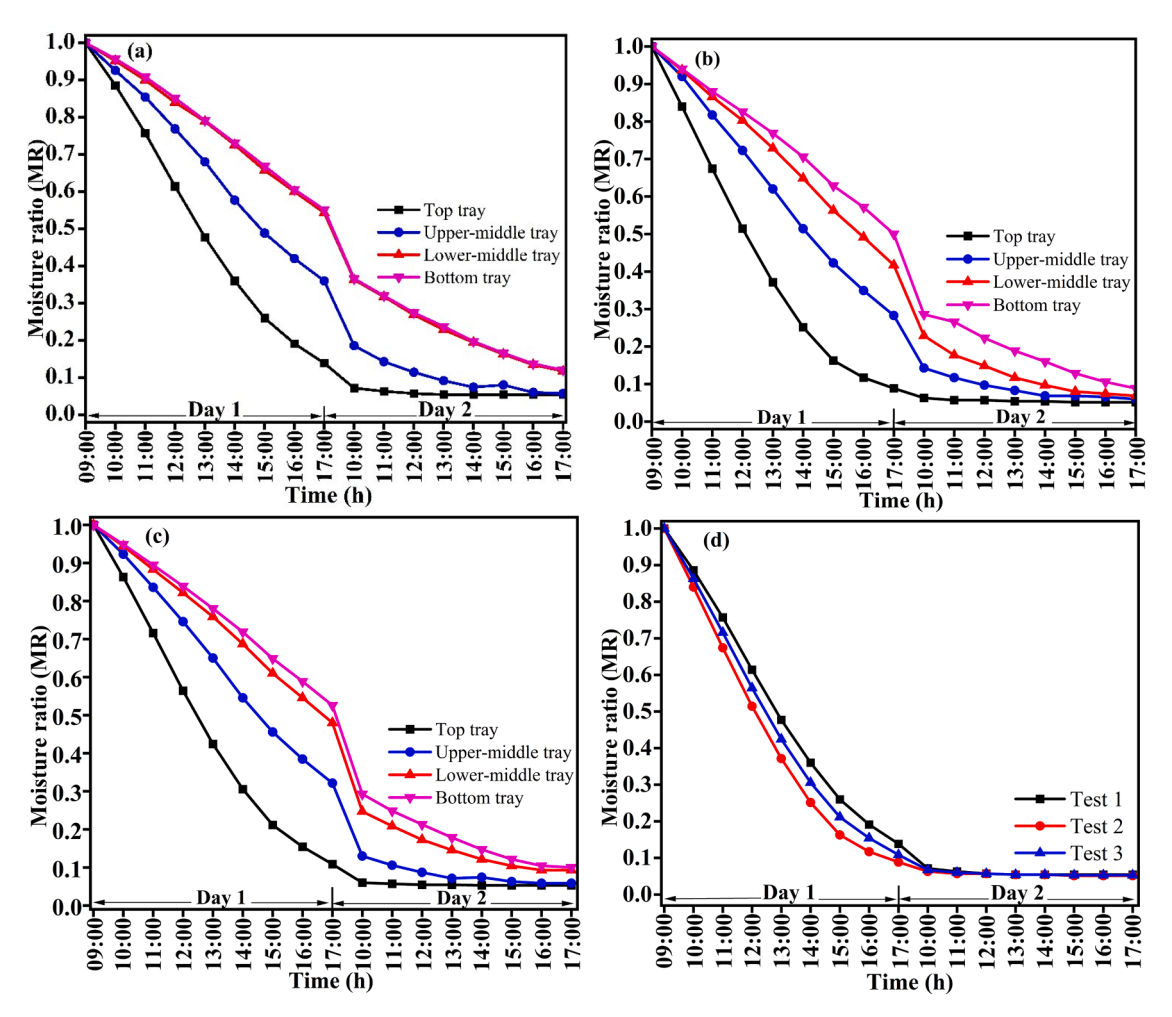


Fig. 7. Moisture ratio of apple slices on (a) test 1, (b) test 2, (c) test 3, and (d) top trays.

reported by Sevik et al. [21], temperature is a significant factor affecting the drying rate by moving water that evaporates from the surface of the product, thus reducing the drying time. On the second day, the increase in the DR at 10:00 am is attributed to the build-up of moisture gathered from apple slices at night. The moisture removal on the top tray is higher compared to that of the bottom trays, thus the values of the DR are higher. The high values of the DR of test 1 can be attributed to both high average airflow velocity and temperature (3.42 m/s and 54.94 °C), compared to test 2 (3.02 m/s and 48.46 °C) and test 3 (2.96 m/s and 47.19 °C).

Mathematical modelling of apple slices

Mathematical modelling is crucial for the design and optimization of the drying process. The experimental data related to the drying of apple slices in 8-hour tests were transformed into a non-dimensional parameter (MR) to standardize the drying with respect to time. To identify an appropriate drying model for apple slices, the current experimental data represented in terms of MR were compared with twelve different empirical models from the literature. The suitability of each model was evaluated based on the highest coefficient of determination (R²) and the lowest values of chi-square (χ^2). Nonlinear regression analyses for three drying tests are detailed in Table 5. Based on these criteria, the Page, Modified Page, Two-term exp, and Verma et al. models were identified as the best fits for the indirect solar drying of apple slices. The R² values for the Page model ranged from 0.9982 to 0.9988, and χ^2 values ranged from 0.00051 to 0.00071. The modified Page model showed R² values from 0.9916 to 0.9945 and χ^2 from 0.00057 to 0.00081. For the Two-term model, R² ranged from 0.9926 to 0.9954, and χ^2 from 0.00069. These models have been effectively used to describe the drying behaviour of apple slices and compared with those obtained in literature, as shown in Table 5.

The results of thin-layer drying models for apple slices using the Page model, which is closer to 1, for tests 1, 2, and 3 are expressed as follows:

$$MR = \exp(-0.1140t^{1.3560}) \tag{17}$$

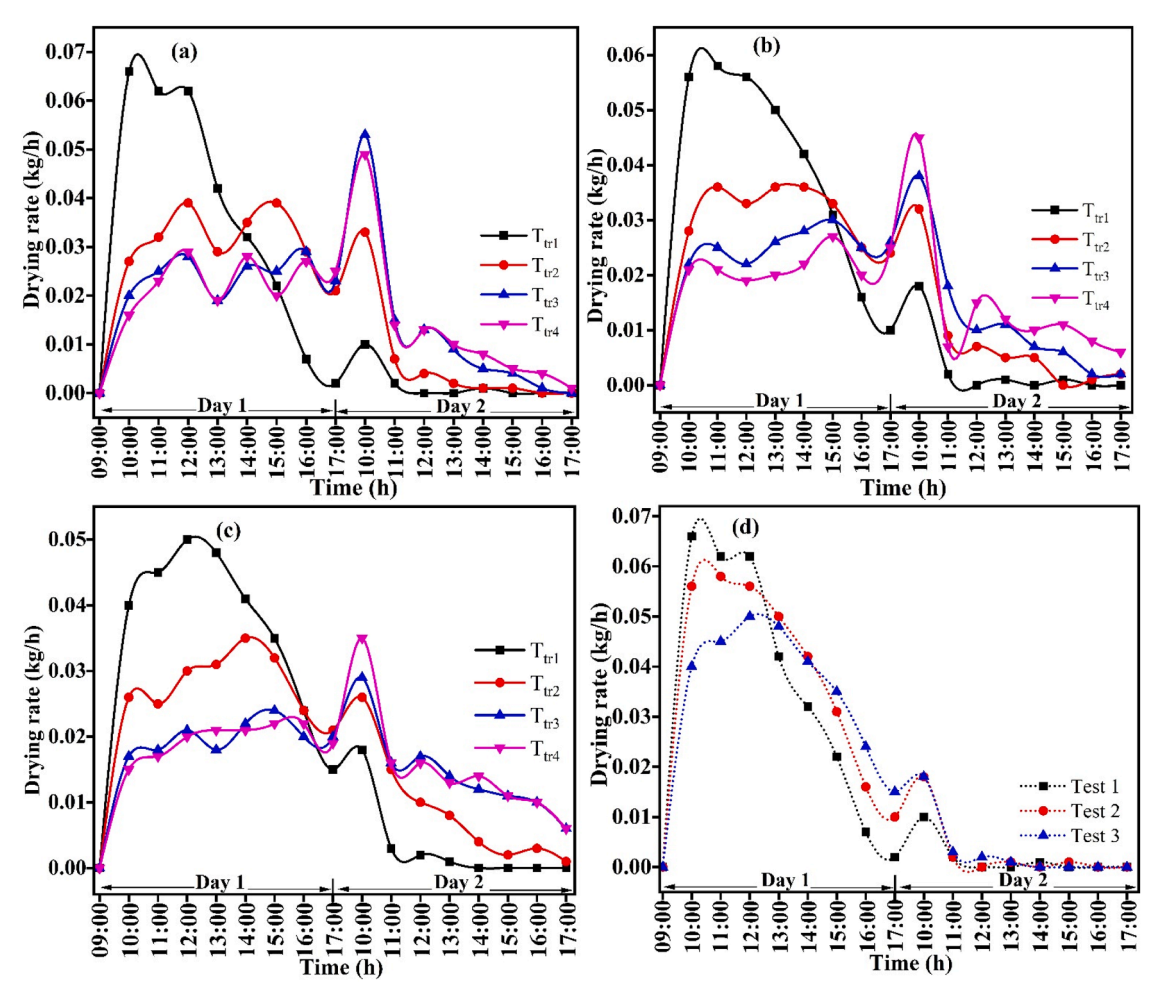


Fig. 8. Drying rates in apple slices of (a) test 1, (b) test 2, (c) test 3, and (d) top trays.

$$MR = \exp(-0.1778t^{1.2403}) \tag{18}$$

$$MR = \exp(-0.1456t^{1.2860}) \tag{19}$$

Fig. 9 illustrates the comparison of experimental and predicted moisture ratio values with the Page model. It is clear from the figure that the Page model accurately predicts the moisture ratio from all the drying tests of apple slices. The findings of the present work identified the Page model as the best fit for predicting MR in apple slices drying. This model is consistent with the work of Lingayat et al. [19] and Atalay [11] who respectively studied the development of indirect solar with a V-shaped absorber plate and solar air heater for the drying of sliced apples. However, different mathematical models were used to describe the drying data of apple slices in the literature, including the Wang-Singh, Midili et al., and Newton as shown in Table 6. Few studies have focused on the monitoring of shrinkage and rehydration ratio, which are important critical metrics to maintain the structural, nutritional, and quality assessment of dried apples. On the other hand, controlling the temperature within the dryer in real-drying conditions may represent an obstacle for subsistence farmers by adding technical adjustments, therefore affecting the drying processes. That is why the portable solar dryer developed in this work operates without controlling any drying parameters. Nonetheless, the drying time of apple slices is higher compared to some of the mentioned research studies (Table 5), hence, suggesting improving the drying components of the next dryer model to significantly reduce this time and broaden the applicability to other fresh products. This is due to the smaller size of the developed prototype because it caters for subsistence farmers. However, more detailed evaluations have been presented in our study compared to previous work.

Effective moisture diffusivity and thermal properties

The graphs of the logarithm of moisture ratios (ln MR) against drying time, illustrated by Fig. 10(a) were plotted to evaluate the effective moisture diffusivities (D_{eff}) of apple slices at different tests. According to recent studies [52], effective diffusivity values lay out within a range of 10^{-9} to 10^{-1} m²/s, whereas Zogzas et al. [53] reported a range of 10^{-8} to 10^{-12} m²/s during the dehydration of

Scientific African 30 (2025) e03012

Table 5Comparison with the drying behaviour of apple slices in the literature.

Drying mode	Apple thickness (mm)	Flow rate (kg/s)	Velocity (m/s)	Drying time (h)	Best fit model	Final MR	RR	Shrinkage (%)	Drying temp. (°C)	$D_{\rm eff}$ (m ² /s)	Refs.
Solar air drying	4.2	0.021-0.061	2.2-4.5	8	N/A	N/A	N/A	N/A	N/A	N/A	[48]
Convective drying	4	N/A	1	1.6	Midili et al.	N/A	N/A	N/A	50–70	$1.95 \times 10^{-7} 4.09 \times 10^{-7}$	[17]
ISD	2.4	0.015-0.025	20-50	N/A	Wang-Singh	< 0.1	N/A	N/A	20-50	N/A	[49]
ISD	5	N/A	0.5	N/A	Page	0.080	N/A	N/A	42-73	4.28×10^{-9}	[19]
Solar tracking system	14	N/A	1.5	13	Midili et al.	N/A	N/A	N/A	55	$10^{-7} - 10^{-6}$	[50]
Hot air drying	4	N/A	1.5	N/A	Midili et al.	N/A	4.527	74.7-82.35	50-70	$10^{-10} - 10^{-9}$	[51]
Solar air heater	5	N/A	N/A	6	Page and Lewis	< 0.1	N/A	N/A	45–55	N/A	[11]
Response surface	5	N/A	N/A		Newton	N/A	1.23	N/A	40.9-65	N/A	
ISD	3.6	Uncontrolled	Uncontrolled	10	Page	0.055	3.03–3.24	41.36–43.2	Uncontrolled	$1.68{\times}10^{-10} 1.89{\times}10^{-10}$	Present study

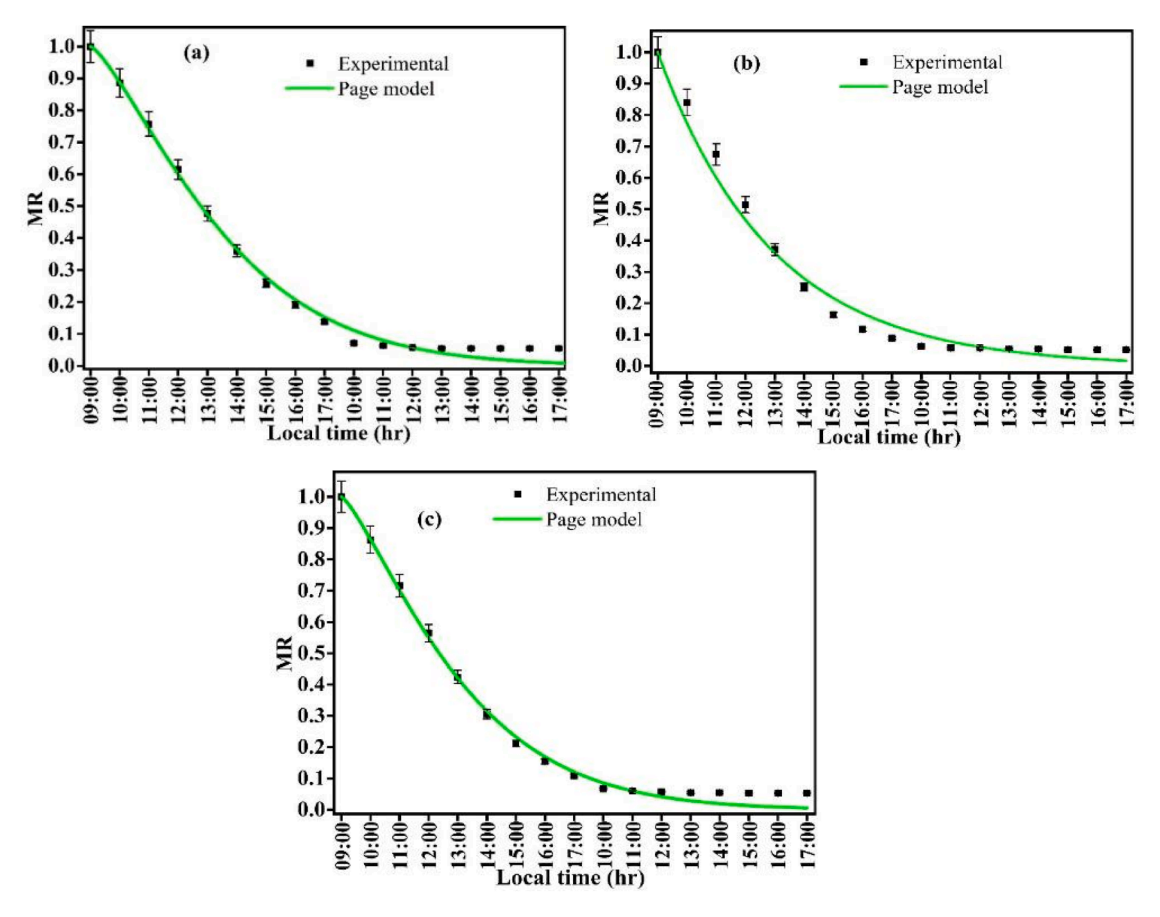


Fig. 9. Comparison of experimental and predicted moisture ratio of Page model.

food products. According to Fick's diffusion model (Eq. (9)), it can be observed that the values of D_{eff} of apple slices were 1.89×10^{-10} , 1.68×10^{-10} , and 1.78×10^{-10} m²/s for tests 1, 2, and 3, respectively, and agree well with the values presented in recent literature. In a study conducted by Lingayat et al. [19]., the effective moisture diffusivity was 4.28×10^{-9} m²/s, while values ranging between 0.713×10^{-10} to 7.66×10^{-10} m²/s were obtained by Beigi et al. [54]. at 30, 45, and 55 °C during drying of apple slices. The higher value of effective moisture diffusivity of test 1 may be attributed to the higher values of solar radiation and wind speed that were 707 W/m² and 3.43 m/s, respectively. As solar radiation increases, apple slices receive more thermal energy that speeds up evaporation and increase apparent moisture diffusivity. On the other hand, the internal moisture moves rapidly to the surface when wind speed increases to reach equilibrium, leading to a higher moisture diffusivity level.

Fig. 10(b) displays the hourly variation of collector efficiencies during three tests in the drying of apple slices using the portable and easily transportable indirect solar dryer. The temperatures of the top trays are selected as outlet temperatures since their drying rates are higher than those of the bottom trays. The collector efficiency values show notable fluctuations, reflecting differences in performance from early morning to mid-morning when solar radiation is generally lower but gradually increases. On day 1 (from 09:00 am to 05:00 pm), test 1 shows relatively high efficiencies, starting at around 10.08 % at 09:00 am, peaking at about 24.21 % at 11:00 am, then fluctuating slightly between 14.58 % at 12:00 pm and 23.48 % at 5:00 pm. Test 2 displays the lowest efficiency, beginning at 5.11 % and rising quickly to about 11.80 % at 11:00 am, then increasing to around 11.97 % at 3:00 pm, and remaining relatively stable with minor fluctuations until 5:00 pm. Compared to test 2, test 3 starts with a higher efficiency of around 8.46 %, peaking at 16.11 %, the highest point during day 1. These results for day 1 indicate that the solar efficiencies of tests 1 perform better in the morning than test 2, confirming the higher solar radiation recorded for test 1 (723.6 W/m²) compared with test 2 (718.2 W/m²) and test 3 (701.7 W/m²). Additionally, the average temperatures were 47.93, 46.74, and 39.03 °C, respectively, aligning well with the reported average solar radiation. On the second day, the solar collector efficiency of test 3 starts moderately high at 12.07 %, then steadily declines throughout the day, reaching nearly 3.86 % at 5:00 pm. This trend is typical of solar drying systems operating under intermittent or low solar radiation (673 W/m²), confirming cloudy conditions. During overcast days, solar radiation can be reflected, absorbed, or scattered in various directions, greatly reducing the amount reaching the drying surface of the apple slices. As cloud cover likely increased or stayed constant, solar radiation decreased, limiting the collector's ability to absorb and convert solar energy effectively. In contrast to test 3, fluctuations and increases in efficiency were observed in test 2 throughout the day, reaching a maximum of 24.86 % at 10:30 am on day 2.

Table 6Fitting results of mathematical models for drying apple slices.

Model names	Tests	Constants		\mathbb{R}^2	χ^2
	1	k = 0.2025		0.9752	0.00261
Newton or Lewis	2	k = 0.2551		0.9836	0.00156
	3	k = 0.2305		0.9814	0.00186
	1	k = 0.1140	n = 1.3560	0.9988	0.00047
Page	2	k = 0.1778	n = 1.2403	0.9982	0.00071
	3	k = 0.1456	n = 1.2860	0.9985	0.00051
	1	k = 0.2025	n = 1.3601	0.9945	0.00057
Modified Page	2	k = 0.2484	n = 1.2400	0.9916	0.00081
	3	k = 0.2235	n = 1.285	0.9936	0.00064
	1	k = 0.2066	a = 1.1026 c = -0.0343	0.9813	0.00197
Henderson-Pabis	2	k = 0.2726	$a = 1.0507 \ c = 0.0058$	0.9848	0.00145
	3	k = 0.2376	a = 1.0717 c = -0.0011	0.9840	0.00160
	1	k = 0.2066	$a = 1.1026 \ c = -0.0343$	0.9813	0.00197
Logarithm	2	k = 0.2726	$a = 1.0507 \ c = -0.0060$	0.9848	0.00145
	3	k = 0.2376	$a = 1.0717 \ c = -0.0105$	0.9840	0.00160
	1	k = -0.0609	$a = 0.9234 \ b = -0.1954 \ n = 1.0945$	0.9524	0.00456
Midili and Kucuk	2	k = -0.0828	$a = 0.9871 \ b = -0.2170 \ n = 0.9911$	0.9852	0.00156
	3	k = -0.0673	$a = 0.9567 \ b = 0.2032 \ n = 1.0576$	0.9726	0.00274
Two-term	1	$k_0 = 0.5399$	$k_1 = 0.2254 \ a = 0.5399 \ b = 0.2254$	0.9777	0.00234
	2	$k_0 = 0.2446$	$k_1 = 0.2446 \ a = 0.5326 \ b = 0.5326$	0.9825	0.00175
	3	$k_0 = 0.2680$	$k_1 = 0.2680 \ a = 0.5267 \ b = 0.5274$	0.9836	0.00157
•	1	k = 0.3156	a = 1.9346	0.9954	0.00048
Two-term exp	2	k = 0.3652	a = 1.8348	0.9926	0.00069
	3	k = 0.3367	a = 1.8754	0.9946	0.00053
	1	k = g = h = 0.2254	$a = c = 0.3599 \ b = 0.36$	0.9737	0.00277
Mod. Henderson	2	k = g = h = 0.2680	$a = c = 0.3520 \ b = 0.3516$	0.9806	0.00186
	3	k = g = h = 0.2445	$a = b = 0.3551 \ c = 0.3548$	0.9793	0.00207
Wang-Singh	1	a = -0.1553	b = 0.0062	0.9932	0.00071
	2	a = -0.1745	b = 0.0076	0.9761	0.00229
	3	a = -0.1651	b = 0.0068	0.9887	0.00110
	1	k = 0.2096	a = b = 1	0.9716	0.00299
Diffusion appr.	2	k = 0.2550	a = b = 1	0.9813	0.00179
**	3	k = 0.1582	a = b = 1	0.9818	0.00182
	1	k = 0.3133	a = 1.8901 $g = 0.6221$	0.9950	0.00052
Verma et al.	2	k = 0.3238	a = 1.3463 $g = 1.0559$	0.9926	0.00069
	3	k = 0.3092	a = 1.4859 $g = 0.8304$	0.9945	0.00054

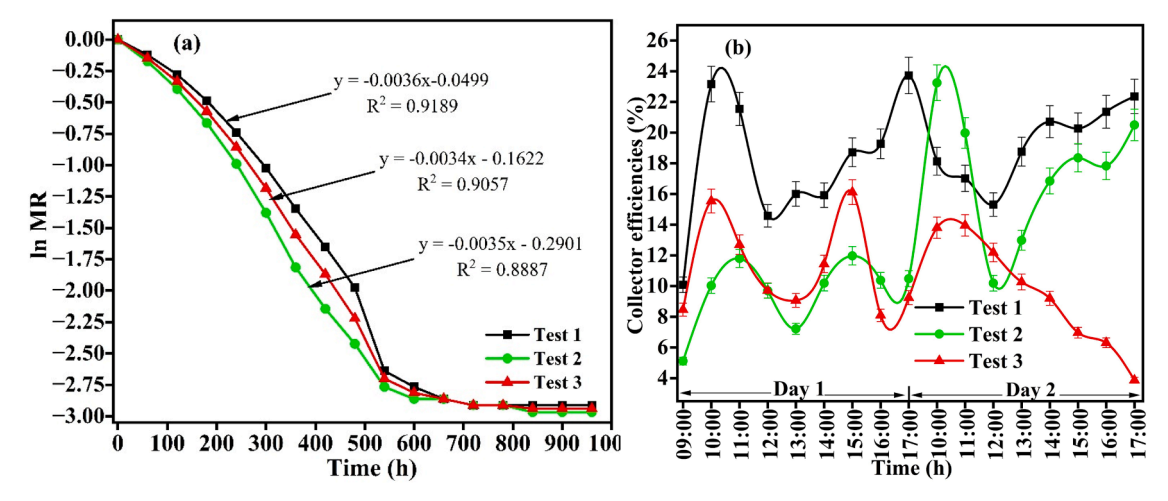


Fig. 10. Variation of (a) ln MR and (b) change of collector efficiencies with time for tests 1, 2, and 3.

Specific heat energy consumption

Time-dependent changes in specific heat consumption for the dehydration of apple slices in tests 1, 2, and 3 during continuous drying days are shown in Fig. 11. SEC values are low and stable across all tests on day 1, ranging from 0.7 to 2.2 kWh/kg, indicating efficient energy use. At the beginning of the drying process and throughout the day, water is more accessible at the surface of the apple slices. Additionally, the recorded solar radiation during the two continuous drying tests was generally high due to weather conditions.

Consequently, lower SEC values occurred because of rapid evaporation. The average SEC values were 1.55, 1.75, and 1.54 kWh/kg for tests 1, 2, and 3, respectively. The lowest SEC values of 0.70, 0.82, and 0.84 kWh/kg were observed at 5:00 pm. Conversely, on day 2, it can be seen a significant increase in SEC values across all tests from 10:00 am, peaking at 3:00 pm for test 2 and at 4:00 pm for tests 1 and 3, with values of 8.31, 12.02, and 15.10 kWh/kg, respectively. As the drying process continues, the drying rate decreases, leading to a rise in SEC. The highest values observed in test 3 may be due to less favourable weather conditions compared to tests 1 and 2. The product loses a significant amount of moisture early in the drying process, which requires more energy and time to remove the remaining moisture. As the moisture content of the product decreases toward the end of the process, the energy required to extract the remaining moisture increases.

Quality assessment

Fig. 12 shows a photograph of apple slices before and after the two consecutive 8-hour drying processes. The dried slices appear smaller, more flexible, chewy, shrunken, and present a noticeable difference in colour, compared to the wet fruits. The rehydration ratio (RR) is used to evaluate the reconstitution attributes of food following the drying process. RR was calculated using 5 g of dried apple slices, and values of 3.10, 3.25, and 3.31 were obtained from tests 1, 2, and 3, respectively. The lower values of the RR may be attributed to the fast drying of the outer layer of dried apple slices, creating a rigid barrier that inhibits water from entering the inner layer. The rehydration coefficients were 3.03, 3.24, and 3.18, indicating effective and relatively consistent drying conditions for removing moisture across all tests. However, the slight variations in values are likely attributed to temperature fluctuations or drying kinetics differences. The current indirect solar dryer effectively produces dried apple slices suitable for later consumption, with minimal structural change. Shrinkage factors (%) in dried apple slices were 43.2, 42.64, and 41.36 % in the respective tests, suggesting nearly uniform drying conditions in the top trays.

Drying apple slices for continuous 32-hour drying tests

Ambient conditions

The dehydration process over a prolonged period is influenced by solar radiation, ambient air temperatures, trays, and the walls of the dryer. Fig. 13 shows the hourly fluctuations of instantaneous solar radiation during all the drying tests on apple slices over 32 h from October 23 - 29, 2024. The weather was mostly sunny throughout this period. It was observed that solar radiation followed a consistent trend across each test, remaining relatively stable and ensuring a favourable drying environment. On the first day, solar radiation started at 507.8 W/m^2 for test 1, 534.9 W/m^2 for test 2, and 638.2 W/m^2 for test 3, reaching peak values of 960.8, 972.1, and 1041 W/m^2 for tests 1, 2, and 3 around 12:30 pm, before declining. The average solar radiation values on day 1 were 646.7, 654.8, and 714.4 W/m^2 . The lowest values, recorded between 6:00 pm on the first day and 6:45 am the next day, across all tests, can be attributed to sunset when irradiance completely disappeared. On the second day, the average values measured were 571.7, 590.8, and 628.9 W/m^2 , with maximum readings of 954.2, 956.2, and 1034.1 W/m^2 around 12:30 pm.

Temperature profiles of the top walls, inside the drying chamber, and the ambient air recorded during 32 h of each drying test are shown in Fig. 14. The data were collected while the DC fans ran continuously throughout the experiments. It is observed that the different trays exhibited clear vertical thermal stratification of temperatures, which significantly affects the drying kinetics. The profiles of each drying test showed a similar trend, with temperatures rising at the beginning of the drying process due to increasing solar radiation. As expected, the top walls reached the highest temperatures, peaking between 57 and 65 °C around midday (1:00 to 2:00 pm), because of direct sunlight exposure. The top wall affects air heating and the temperature gradient within the dryer. As a

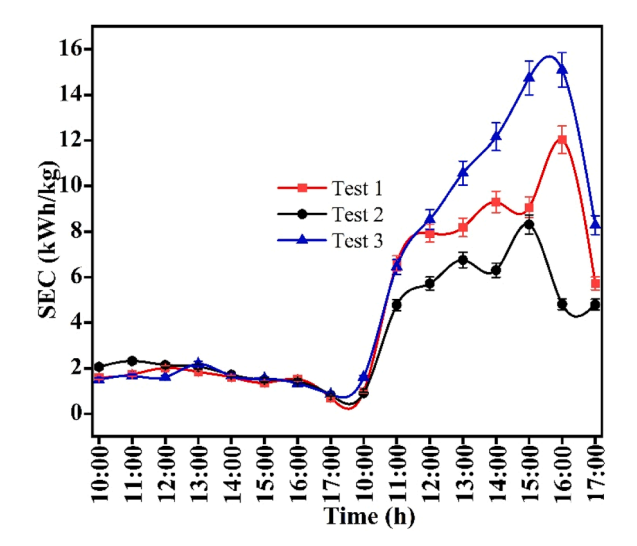


Fig. 11. Hourly variation of SEC versus time of tests 1, 2, and 3.

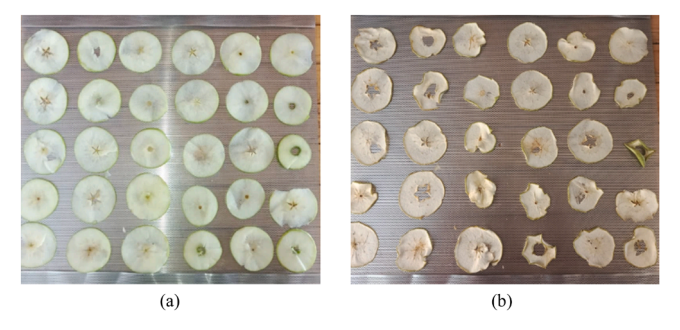


Fig. 12. Snapshot of apple slices of (a) before and (b) after the drying process.

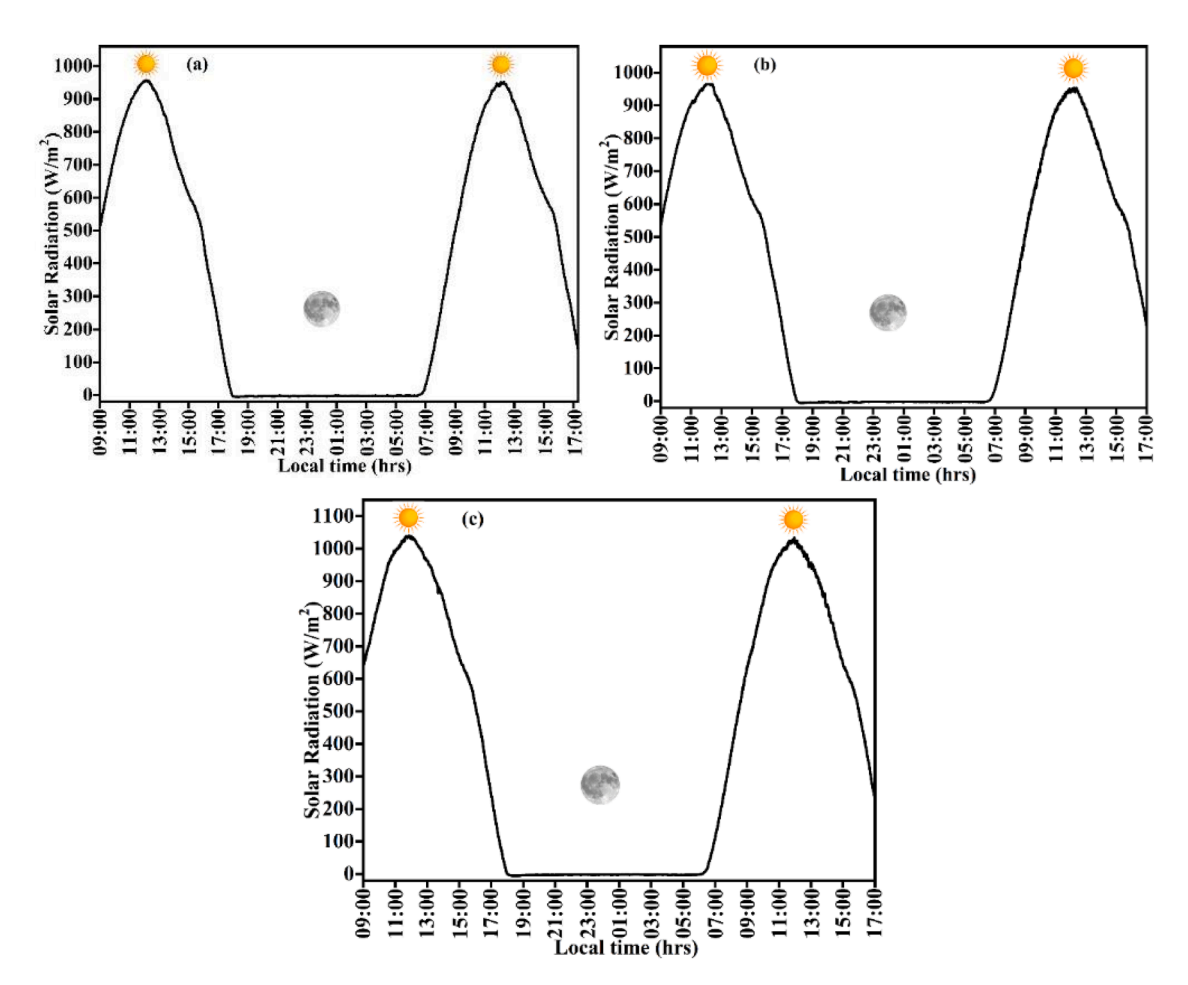


Fig. 13. Variation in solar radiation and ambient temperature during (a) test 1, (b) test 2, and (c) test 3.

result, less dense warm air rises and gathers near the top of the dryer, causing higher thermal exposure for the top and upper-middle trays, peaking at about 54–60 °C and 52–54 °C, respectively. These trays constitute the hottest zone, leading to an accelerated evaporation rate of apple slices and a reduction in drying time. The thermal behaviour of T_{tr2} is slightly lower than T_{tr1} , likely due to airflow dynamics and moisture removal from partially dried apple slices. Conversely, T_{tr3} shows moderately higher temperatures, peaking at 52–54 °C, remaining cooler than the upper trays but warmer than T_{tr4} . These trays are in the lowest and slowest zones, with more variability, possibly due to airflow fluctuations, moisture content, and humidity released from the trays above, resulting in a slower drying process. The ambient temperature peaked around 31–33 °C on the first day but remained lower than the temperatures of the trays, reinforcing the solar dryer's capability to maintain an internal environment optimal for faster drying of apple slices. It is noted that the temperature profiles of T_{amb} are higher than those of the dryer components during nighttime. The lower temperature of T_{tw} at night likely results from its radiative cooling property, as it is made of polycarbonate material that loses heat by emitting long-

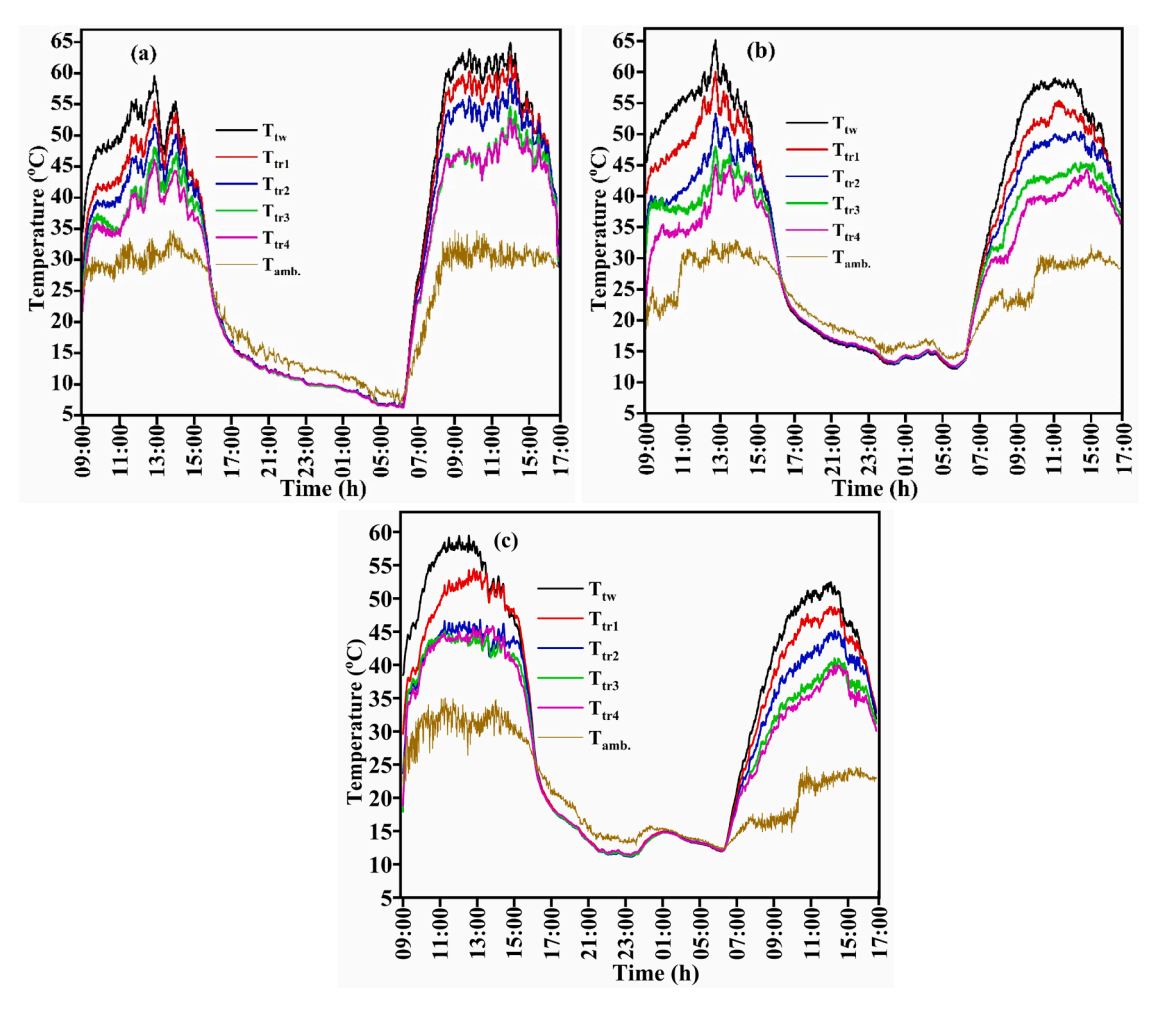


Fig. 14. Temperature changes in top walls, trays, and ambient air in 32-hour tests.

wave infrared radiation. Meanwhile, a thin, uninsulated stainless-steel dryer with a low thermal mass tends to lose heat at night and quickly cools down below ambient temperature. Metal components lose stored heat during the day through convection to the surrounding air inside the dryer. Lastly, since the solar dryer is a passive system without any storage material, it cannot sustain elevated temperatures once solar input stops. On the following day, starting at 07:00 am, similar patterns in T_{tw} , T_{tr1} , T_{tr2} , T_{tr3} , and T_{amb} were observed. These drawbacks can be catered by using insulation, improving air circulation, and adding thermal energy storage at the expense of increasing the cost.

The variation in temperature of the left, right, back walls, and ambient air over the 32-hour continuous drying tests is shown in Fig. 15. In all tests, discontinuities and sudden jumps in temperature were observed, likely due to changing weather conditions, including cloudiness of the air. Similar observations were reported by Yazici et al. [55] during the comparative study of drying okra with geothermal and solar hybrid forced convection indirect-type cabinet dryers. From 9:00 am to 11:30 pm, the right and back walls, which faced sunlight, heated up faster and more intensely due to solar radiation reaching the dryer, resulting in higher temperatures compared to the left wall across all tests. Because sunlight hits the dryer at varying angles and intensities, walls more directly exposed to sunlight heat up more. At noon, as sunlight becomes more vertical, to around 5:30 pm, the left wall receives more solar radiation, causing it to aachieve the hottest temperature, which then decreases as the right wall enters the shade with lower recorded temperatures. The maximum temperatures recorded in all walls were 62.5 °C for the left wall, 58.6 °C for the back wall, and 48.2 °C for the right wall in test 1, after which they started declining. On the second day, from 7:00 am to 5:00 pm, the same trends were observed, with maximum temperatures of 63.2 °C, 50.5 °C, and 57.4 °C for the left, back, and right walls, respectively, with the peak at 3:00 pm.

According to the continuous drying of apple slices (Fig. 4), the maximum relative humidity was obtained after one hour of the drying process. In the 32-hour consecutive drying process, maximum values of 69, 71, and 73 were obtained for tests 1, 2, and 3, respectively, and a final value around 16 % confirming that the apple slices were fully dried.

Drying kinetics and performance analysis in 32-hour drying test

The moisture ratio of T_{tr1}, T_{tr2}, T_{tr3}, and T_{tr4} versus drying time is shown in Fig. 16. As expected, the top tray exhibited the lowest

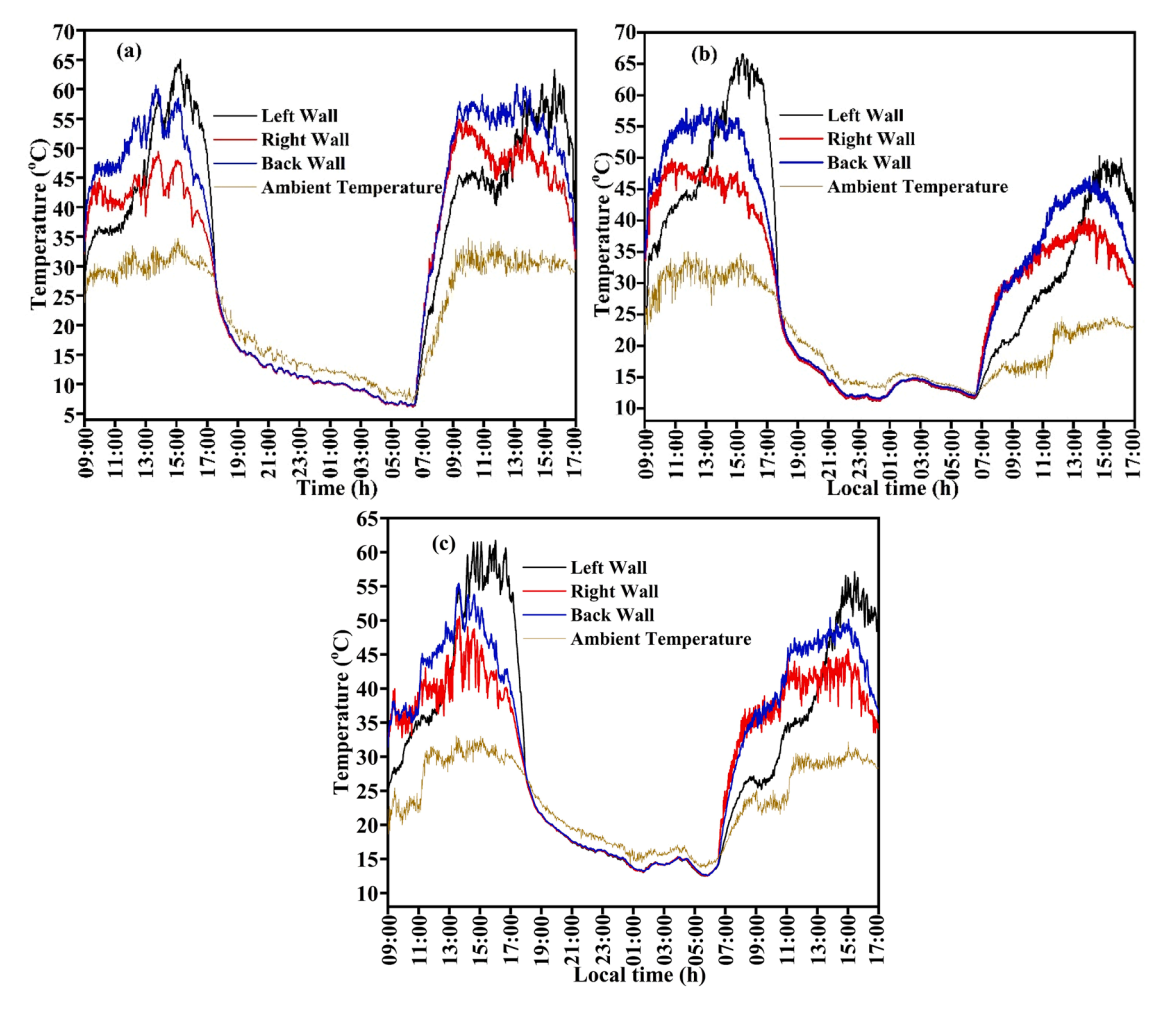


Fig. 15. Temperature profiles of walls during 32-hour in (a) test 1, (b) test 2, and (c) test 3.

MR compared to other trays due to its position near the top wall, obtaining the highest temperature throughout the drying process. The values of 0.1029, 0.0971, and 0.0857 for T_{tr1} were obtained on the top trays during tests 1, 2, and 3, while values of 0.1229, 0.0071, and 0.1086 were obtained from the bottom trays. This vertical stratification of MR could also be attributed to the difference in average solar radiation hitting the solar dryer over the 32-hour test. The calculated values were 371.2, 374.5, and 416.2 W/m² for tests 1, 2,

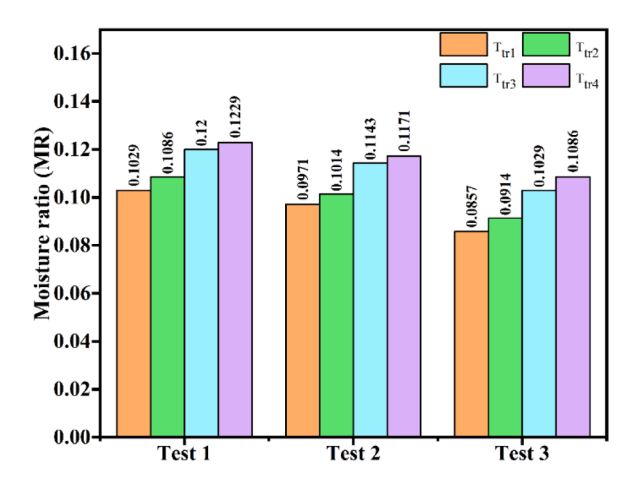


Fig. 16. Moisture ratio of apple slices on top, upper-middle, lower-middle, and bottom trays in 32-hour test.

and 3, respectively. The values of specific energy consumption (SEC) were 10.30, 10.86, and 11.38 kWh/kg for tests 1, 2, and 3. The close values of tests 1 and 2 may be attributed to the average values of recorded solar radiation of 370.1 and 373.8 W/m 2 , whereas a value of 416.2 W/m 2 was obtained for test 3.

Conclusion

In this work, a novel portable solar dryer was employed for dehydration of apple slices in consecutive (8-hour, in day) and continuous (32-hour, day and night) drying tests in sunny and cloudy conditions. The novelty of this study lies in the design of a portable, easily transportable, and low-cost solar dryer manufactured from locally available materials, operating in real-time conditions, particularly benefiting subsistence farmers living in off-grid rural areas, which can do both solar drying during sunshine hours and continuous overnight drying for 32 h. The drying and performance characteristics were evaluated for both 8-hour tests on two days and continuous overnight 32-hour tests. The findings highlighted the significant influence of solar radiation, with average values of 718.2, 723.6, and 701.7 W/m² in 8-hour tests, while the average values were 370.1, 373.8, and 416.2 W/m² in the 32-hour drying tests. The maximum temperatures obtained in the top tray of the dryer were 63.33, 59.23, and 53.6 °C, respectively, for consecutive 8hour tests, while maximum temperatures of 65.02, 59.72, and 65.21 °C were recorded for continuous tests. The dryer temperatures were stratified from the top to the bottom tray. The temperature profiles of the walls changed according to their exposure to sunlight, thereby playing an important role in maintaining the thermal energy within the drying cabinet. It was found that the cloudy day conditions on day 2 of test 3 in the 8-hour test increased the drying time to 10.5 h, whereas for tests 1 and 2, the drying time was around 10 h. The average drying rates were 0.050, 0.058, and 0.066 kg/h, while effective moisture diffusivities were 1.89×10^{-10} . 1.68×10^{-10} , and 1.78×10^{-10} m²/s for the consecutive drying tests. The hourly opening and closing of the dryer deeply affected the collector efficiency in the 8-hour tests. The maximum collector efficiencies of day 1 were 24.21, 11.80, and 16.11 % for tests 1, 2, and 3, respectively. Maximum values of specific energy consumption were 8.31, 12.02, and 15.10 kWh/kg for the 8-hour test; while, values of 10.30, 10.86, and 11.38 kWh/kg for the 32-hour test were comparable because of the comparable average solar radiation conditions. The insulation of walls or the use of storage materials to minimize energy losses, the use of larger perforated trays, and exergy and economic analyses will be investigated to improve the performance and drying kinetics. Additionally, upscaling the components of the dryer and broadening its applicability to a wide range of agricultural products will substantially address post-harvest losses, strengthen rural economies, and promote small-scale agricultural processing. Future work will also be aimed at addressing the thermal stratification in the trays and attempting to uniformize the drying temperatures in the whole drying chamber. The authors are currently developing a new prototype that will dry uniformly in all trays. A computational fluid dynamics (CFD) model to understand the heat and mass transfer in the dryer will also be part of future work.

Credit authorship contribution statement

Patrick Tsopbou Ngueagni: Investigation, Conceptualization, Methodology, Formal analysis, Writing –original draft. Ashmore Mawire: Investigation, Conceptualization, Methodology, Writing – review & editing, Formal analysis, Supervision

Declaration of competing interest

The authors declare that they have no known competing financial interests or personal relationships that could have appeared to influence the work reported in this paper.

Acknowledgement

The authors are grateful to the North-West University, South Africa, for the financial support for the postdoctoral research fellowship through the funding NM.G01487.

References

- [1] X.-M. Fang, et al., Performance assessment of an evacuated tube solar-electric hybrid dryer for lotus seeds drying: moisture removal behavior, GHG emission and thermodynamic analysis, J. Clean. Prod 406 (2023) 136972, https://doi.org/10.1016/j.jclepro.2023.136972. Jun.
- [2] H.U. Rehman, F. Naseer, H.M. Ali, An experimental case study of solar food dryer with thermal storage using phase change material, Case. Stud. Therm. Eng. 51 (2023) 103611, https://doi.org/10.1016/j.csite.2023.103611. Nov.
- [3] M. Goud, M.V.V. Reddy, V.P. Chandramohan, S. Suresh, A novel indirect solar dryer with inlet fans powered by solar PV panels: drying kinetics of Capsicum Annum and Abelmoschus esculentus with dryer performance, Sol. Energy 194 (2019) 871–885, https://doi.org/10.1016/j.solener.2019.11.031. Dec.
- [4] R. Zhu, et al., Combined calcium pretreatment and ultrasonic/microwave drying to dehydrate black chokeberry: novel mass transfer modeling and metabolic pathways of polyphenols, Innov. Food. Sci. Emerg. Technol. 83 (2023) 103215, https://doi.org/10.1016/j.ifset.2022.103215. Jan.
- [5] N.A. Mhd Safri, et al., Current status of solar-assisted greenhouse drying systems for drying industry (food materials and agricultural crops), Trends. Food. Sci. Technol 114 (2021) 633–657, https://doi.org/10.1016/j.tifs.2021.05.035. Aug.
- [6] A. Mawire, M. Ramokali, M. Mothupi, M. Vanierschot, An experimental evaluation of drying banana slices using a novel indirect solar dryer under variable conditions, Heliyon 10 (7) (2024) e28268, https://doi.org/10.1016/j.heliyon.2024.e28268. Apr.
- [7] M. Mohanraj, P. Chandrasekar, Drying of copra in a forced convection solar drier, Biosyst. Eng 99 (4) (2008) 604–607, https://doi.org/10.1016/j. biosystemseng.2007.12.004. Apr.
- [8] M. Sharma, D. Atheaya, A. Kumar, Performance evaluation of indirect type domestic hybrid solar dryer for tomato drying: thermal, embodied, economical and quality analysis, Therm. Sci. Eng. Prog. 42 (2023), https://doi.org/10.1016/j.tsep.2023.101882. Jul.

- [9] F. Ullah, K. Hasrat, S. Iqbal, S. Kumar, M. Mu, S. Wang, Performance evaluation of improved indirect flat-plate solar collector drier with integrated phase change material for drying kiwifruit (Actinidia deliciosa A. chev.), J. Stored. Prod. Res 111 (2025) 102551, https://doi.org/10.1016/j.jspr.2025.102551. May.
- [10] Y. Rahmani, R. Khama, Improving open sun and indirect solar drying kinetics with physicochemical quality of regal seedless grapes by novel pretreatment solution, J. Stored. Prod. Res 106 (2024) 102292, https://doi.org/10.1016/j.jspr.2024.102292. May.
- [11] H. Atalay, M. Turhan Çoban, O. Kıncay, Modeling of the drying process of apple slices: application with a solar dryer and the thermal energy storage system, Energy 134 (2017) 382–391, https://doi.org/10.1016/j.energy.2017.06.030. Sep.
- [12] O. Badaoui, A. Djebli, S. Hanini, Solar drying of apple and orange waste: evaluation of a new thermodynamic approach, and characterization analysis, Renew. Energy 199 (2022) 1593–1605, https://doi.org/10.1016/j.renene.2022.09.098. Nov.
- [13] H. Kidane, I. Farkas, J. Buzás, Performance evaluation of solar drying chambers and drying kinetics of apple slices, Energy. Rep. 13 (2025) 4528–4540, https://doi.org/10.1016/j.egyr.2025.04.016. Jun.
- [14] T. Seerangurayar, A.M. Al-Ismaili, L.H. Janitha Jeewantha, A. Al-Nabhani, Experimental investigation of shrinkage and microstructural properties of date fruits at three solar drying methods, Sol. Energy 180 (2019) 445–455, https://doi.org/10.1016/j.solener.2019.01.047. Mar.
- [15] F. Salehi, R. Cheraghi, M. Rasouli, Mass transfer kinetics (soluble solids gain and water loss) of ultrasound-assisted osmotic dehydration of apple slices, Sci. Rep 12 (1) (2022), https://doi.org/10.1038/s41598-022-19826-w. Dec.
- [16] N. WANG, J. Wolf, F. ZHANG, Towards sustainable intensification of apple production in China yield gaps and nutrient use efficiency in apple farming systems, J. Integr. Agric 15 (4) (2016) 716–725, https://doi.org/10.1016/S2095-3119(15)61099-1. Apr.
- [17] V.R. Sharabiani, M. Kaveh, R. Abdi, M. Szymanek, W. Tanaś, Estimation of moisture ratio for apple drying by convective and microwave methods using artificial neural network modeling, Sci. Rep 11 (1) (2021), https://doi.org/10.1038/s41598-021-88270-z. Dec.
- [18] H.S. El-Mesery, K. Ashiagbor, Z. Hu, W.G. Alshaer, A novel infrared drying technique for processing of apple slices: drying characteristics and quality attributes, Case. Stud. Therm. Eng. 52 (2023) 103676, https://doi.org/10.1016/j.csite.2023.103676. Dec.
- [19] A. Lingayat, V.P. Chandramohan, V.R.K. Raju, A. Kumar, Development of indirect type solar dryer and experiments for estimation of drying parameters of apple and watermelon, Therm. Sci. Eng. Prog. 16 (2020) 100477, https://doi.org/10.1016/j.tsep.2020.100477. May.
- [20] H. Kidane, I. Farkas, J. Buzás, Mathematical modelling of golden apple drying and performance evaluation of solar drying systems using energy and exergy approach, Sci. Rep 15 (1) (2025), https://doi.org/10.1038/s41598-025-92133-2. Dec.
- [21] S. Şevik, M. Aktaş, E.C. Dolgun, E. Arslan, A.D. Tuncer, Performance analysis of solar and solar-infrared dryer of mint and apple slices using energy-exergy methodology, Sol. Energy 180 (2019) 537–549, https://doi.org/10.1016/j.solener.2019.01.049. Mar.
- [22] A. Hazervazifeh, A.M. Nikbakht, P.A. Moghaddam, Novel hybridized drying methods for processing of apple fruit: energy conservation approach, Energy 103 (2016) 679–687, https://doi.org/10.1016/j.energy.2016.03.012. May.
- [23] S.R. Shewale, D. Rajoriya, H.U. Hebbar, Low humidity air drying of apple slices: effect of EMR pretreatment on mass transfer parameters, energy efficiency and quality, Innov. Food. Sci. Emerg. Technol. 55 (2019) 1–10, https://doi.org/10.1016/j.ifset.2019.05.006. Jul.
- [24] A.K. Bhardwaj, R. Kumar, S. Kumar, B. Goel, R. Chauhan, Energy and exergy analyses of drying medicinal herb in a novel forced convection solar dryer integrated with SHSM and PCM, Sustain. Energy. Technol. Assess. 45 (2021) 101119, https://doi.org/10.1016/j.seta.2021.101119. Jun.
- [25] A.K. Bhardwaj, R. Kumar, R. Chauhan, Experimental investigation of the performance of a novel solar dryer for drying medicinal plants in Western Himalayan region, Sol. Energy 177 (2019) 395–407, https://doi.org/10.1016/j.solener.2018.11.007. Jan.
- [26] A.K. Bhardwaj, R. Chauhan, R. Kumar, M. Sethi, A. Rana, Experimental investigation of an indirect solar dryer integrated with phase change material for drying valeriana jatamansi (medicinal herb), Case. Stud. Therm. Eng. 10 (2017) 302–314, https://doi.org/10.1016/j.csite.2017.07.009. Sep.
- [27] A. Djebli, S. Hanini, O. Badaoui, B. Haddad, A. Benhamou, Modeling and comparative analysis of solar drying behavior of potatoes, Renew. Energy 145 (2020) 1494–1506. https://doi.org/10.1016/j.renene.2019.07.083. Jan.
- [28] H. Ibrahim, Performance of two terms exponential model on the drying kinetics of solar-dried tomatoes (Lycopersicum esculentum L.) treated with and without chemical preservatives, Egypt. J. Chem (2021), https://doi.org/10.21608/ejchem.2021.93566.4414 vol. 0, no. 0, pp. 0–0, Sep.
- [29] S. Vijayan, T.V. Arjunan, A. Kumar, Mathematical modeling and performance analysis of thin layer drying of bitter gourd in sensible storage based indirect solar dryer, Innov. Food. Sci. Emerg. Technol. 36 (2016) 59–67, https://doi.org/10.1016/j.ifset.2016.05.014. Aug.
- [30] A. Lopez, A. Iguaz, A. Esnoz, P. Virseda, Thin-layer drying behaviour of vegetable wastes from wholesale market, Dry. Technol. 18 (4–5) (2000) 995–1006, https://doi.org/10.1080/07373930008917749. Apr.
- [31] J.R. O'Callaghan, D.J. Menzies, P.H. Bailey, Digital simulation of agricultural drier performance, J. Agric. Eng. Res. 16 (3) (1971) 223–244, https://doi.org/10.1016/S0021-8634(71)80016-1. Sep.
- [32] Q. Zhang, J.B. Litchfield, An optimization of intermittent corn drying in a laboratory scale thin layer dryer, Dry. Technol. 9 (2) (1991) 383–395, https://doi.org/10.1080/07373939108916672. Mar.
- [33] M. Özdemir, Y.O. Devres, The thin layer drying characteristics of hazelnuts during roasting, J. Food. Eng 42 (4) (1999) 225–233, https://doi.org/10.1016/S0260-8774(99)00126-0. Dec.
- [34] H. Atalay, Performance analysis of a solar dryer integrated with the packed bed thermal energy storage (TES) system, Energy 172 (2019) 1037–1052, https://doi.org/10.1016/j.energy.2019.02.023. Apr.
- [35] K. Sacilik, A.K. Elicin, The thin layer drying characteristics of organic apple slices, J. Food. Eng 73 (3) (2006) 281–289, https://doi.org/10.1016/j. ifoodeng.2005.03.024. Apr.
- [36] A. Midilli, H. Kucuk, Z. Yapar, A new model for single-layer drying, Dry. Technol. 20 (7) (2002) 1503-1513, https://doi.org/10.1081/DRT-120005864. Jul.
- [37] P.S. Madamba, R.H. Driscoll, K.A. Buckle, The thin-layer drying characteristics of garlic slices, J. Food. Eng 29 (1) (1996) 75–97, https://doi.org/10.1016/0260-8774(95)00062-3. Jul.
- [38] V.T. Karathanos, Determination of water content of dried fruits by drying kinetics, J. Food. Eng 39 (4) (1999) 337–344, https://doi.org/10.1016/S0260-8774 (98)00132-0. Mar.
- [39] H. Essalhi, M. Benchrifa, R. Tadili, M.N. Bargach, Experimental and theoretical analysis of drying grapes under an indirect solar dryer and in open sun, Innov. Food. Sci. Emerg. Technol. 49 (2018) 58–64, https://doi.org/10.1016/j.ifset.2018.08.002. Oct.
- [40] C. Ertekin, O. Yaldiz, Drying of eggplant and selection of a suitable thin layer drying model, J. Food. Eng 63 (3) (2004) 349–359, https://doi.org/10.1016/j.jfoodeng.2003.08.007. Aug.
- [41] L.R. Verma, R.A. Bucklin, J.B. Endan, F.T. Wratten, Effects of drying air parameters on rice drying models, Trans. ASAE 28 (1) (1985) 296–301, https://doi.org/10.13031/2013.32245.
- [42] A.B. Lingayat, V.P. Chandramohan, V.R.K. Raju, V. Meda, A review on indirect type solar dryers for agricultural crops Dryer setup, its performance, energy storage and important highlights, Appl. Energy 258 (2020) 114005, https://doi.org/10.1016/j.apenergy.2019.114005. Jan.
- [43] A.K. Bhardwaj, R. Kumar, R. Chauhan, S. Kumar, Experimental investigation and performance evaluation of a novel solar dryer integrated with a combination of SHS and PCM for drying chilli in the Himalayan region, Therm. Sci. Eng. Prog. 20 (2020) 100713, https://doi.org/10.1016/j.tsep.2020.100713. Dec.
- [44] A. Srivastava, A. Sharma, A. Kumar, Performance evaluation of indirect solar drying system for potato slices: comparative analysis with open-sun drying method, Sol. Energy 285 (2025) 113114, https://doi.org/10.1016/j.solener.2024.113114. Jan.
- [45] T. Hadibi, et al., Drying characteristic, sustainability, and 4E (energy, exergy, and enviro-economic) analysis of dried date fruits using indirect solar-electric dryer: an experimental investigation, Renew. Energy 218 (2023) 119291, https://doi.org/10.1016/j.renene.2023.119291. Dec.
- [46] A. Kushwah, A. Kumar, M. Kumar Gaur, P. Shrivastava, Environmental sustainability and exergetic based sustainability indicators for heat exchanger-evacuated tube assisted drying system (HE-ETADS), Sustain. Energy. Technol. Assess. 57 (2023) 103277, https://doi.org/10.1016/j.seta.2023.103277. Jun.
- [47] M. Naniwadekar, S. Walke, M. Mandake, R. Tapre, K. Patil, S. Komble, A comprehensive study of performance metrices and potato dehydration at various slice thickness using an IoT-based indirect solar dryer: an experimental approach, Sol. Energy 288 (2025) 113269, https://doi.org/10.1016/j.solener.2025.113269. Mar.

- [48] A. Hassan, A.M. Nikbahkt, Z. Welsh, P. Yarlagadda, S. Fawzia, A. Karim, Experimental and thermodynamic analysis of solar air dryer equipped with V-groove double pass collector: techno-economic and exergetic measures, Energy. Convers. Manag.:. X 16 (2022) 100296, https://doi.org/10.1016/j.ecmx.2022.100296. Dec.
- [49] L. Blanco-Cano, A. Soria-Verdugo, L.M. Garcia-Gutierrez, U. Ruiz-Rivas, Modeling the thin-layer drying process of Granny Smith apples: application in an indirect solar dryer, Appl. Therm. Eng 108 (2016) 1086–1094, https://doi.org/10.1016/j.applthermaleng.2016.08.001. Sep.
- [50] M. Das, E.K. Akpinar, Determination of thermal and drying performances of the solar air dryer with solar tracking system: apple drying test, Case. Stud. Therm. Eng. 21 (2020) 100731, https://doi.org/10.1016/j.csite.2020.100731. Oct.
- [51] M. Beigi, Hot air drying of apple slices: dehydration characteristics and quality assessment, Heat. Mass. Transf./Waerme-. Stoffuebertragung 52 (8) (2016) 1435–1442, https://doi.org/10.1007/s00231-015-1646-8. Aug.
- [52] A. Maskan, S. Kaya, M. Maskan, Hot air and sun drying of grape leather (pestil), J. Food. Eng 54 (1) (2002) 81–88, https://doi.org/10.1016/S0260-8774(01) 00188-1. Aug.
- [53] N.P. Zogzas, Z.B. Maroulis, D. Marinos-Kouris, Moisture diffusivity data compilation in foodstuffs, Dry. Technol. 14 (10) (1996) 2225–2253, https://doi.org/10.1080/07373939608917205. Jan.
- [54] M. Beigi, Influence of drying air parameters on mass transfer characteristics of apple slices, Heat. Mass. Transf./Waerme-. Stoffuebertragung 52 (10) (2016) 2213–2221, https://doi.org/10.1007/s00231-015-1735-8. Oct.
- [55] M. Yazici, R. Kose, S.D. Acer, Investigation of the comparative okra drying performance of a geothermal and solar hybrid forced convection indirect type cabinet dryer, Renew. Energy 239 (2025) 122031, https://doi.org/10.1016/j.renene.2024.122031. Feb.